

Experimental and Theoretical Studies of the Photophysical Properties of 2- and 2,7-Functionalized Pyrene Derivatives

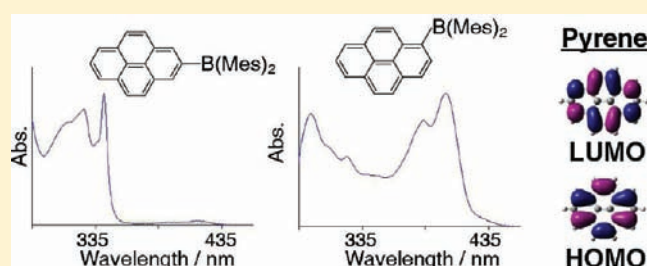
Andrew G. Crawford,[†] Austin D. Dwyer,[†] Zhiqiang Liu,^{†,‡} Andreas Steffen,[†] Andrew Beeby,^{*,†} Lars-Olof Pålsson,[†] David J. Tozer,^{*,†} and Todd B. Marder^{*,†}

[†]Department of Chemistry, Durham University, South Road, Durham DH1 3LE, United Kingdom

[‡]State Key Lab of Crystal Materials, Shandong University, 27 Shanda South Road, Jinan 250100, China

 Supporting Information

ABSTRACT: Pyrene derivatives substituted at the 2- and 2,7-positions are shown to display a set of photophysical properties different from those of derivatives substituted at the 1-position. It was found that, in the 2- and 2,7-derivatives, there was little influence on the $S_2 \leftarrow S_0$ excitation, which is described as “pyrene-like”, and a strong influence on the $S_1 \leftarrow S_0$ excitation, which is described as “substituent-influenced”. In contrast, the 1-substituted derivatives display a strong influence on both the $S_1 \leftarrow S_0$ and the $S_2 \leftarrow S_0$ excitations. These observations are rationalized by considering the nature of the orbitals involved in the transitions. The existence of a nodal plane passing through the 2- and 7-positions, perpendicular to the molecular plane in the HOMO and LUMO of pyrene, largely accounts for the different behavior of derivatives substituted at the 2- and 2,7-positions. Herein, we report the photophysical properties of a series of 2-R-pyrenes {R = C₃H₆CO₂H (1), Bpin (2; pin = OCMe₂CMe₂O), OC₃H₆CO₂H (3), O(CH₂)₁₂Br (4), C≡CPh (5), C₆H₄-4-CO₂Me (6), C₆H₄-4-B(Mes)₂ (7), B(Mes)₂ (8)} and 2,7-R₂-pyrenes {R = Bpin (9), OH (10), C≡C(TMS) (11), C≡CPh (12), C≡C-C₆H₄-4-B(Mes)₂ (13), C≡C-C₆H₄-4-NMe₂ (14), C₆H₄-4-CO₂C₈H₁₇ (15), N(Ph)-C₆H₄-4-OMe (16)} whose syntheses are reported elsewhere. Furthermore, we compare their properties to those of several related 1-R-pyrene derivatives {R = C₃H₆CO₂H (17), Bpin (18), C≡CPh (19), C₆H₄-4-B(Mes)₂ (20), B(Mes)₂ (21)}. For all derivatives, modest (0.19) to high (0.93) fluorescence quantum yields were observed. For the 2- and 2,7-derivatives, fluorescence lifetimes exceeding 16 ns were measured, with most being ca. 50–80 ns. The 4-(pyren-2-yl)butyric acid derivative (1) has a long fluorescence lifetime of 622 ns, significantly longer than that of the commercially available 4-(pyren-1-yl)butyric acid (17). In addition to measurements of absorption and emission spectra and fluorescence quantum yields and lifetimes, time-dependent density functional theory calculations using the B3LYP and CAM-B3LYP functionals were also performed. A comparison of experimental and theoretically calculated wavelengths shows that both functionals were able to reproduce the trend in wavelengths observed experimentally.



INTRODUCTION

Pyrene is an important and well-studied chromophore; its long-lived fluorescence and propensity to form fluorescent excimers via $\pi-\pi$ interactions both in solution and in the solid state have led to its use in a wide variety of applications. For example, pyrene-labeled nucleotide bases are used to study DNA charge transfer,² hybridization of DNA and RNA,^{3–5} and non-covalent interactions between nucleotides,⁶ for polyfluorophore labeling,⁷ and for defect detection.^{8,9} The high sensitivity of the vibronic fine structure of pyrene fluorescence to changes in environment (Ham effect), and the long fluorescence lifetime of pyrene derivatives, allows them to be used as a fluorescent probe.¹⁰ In particular, 4-(pyren-1-yl)butyric acid (17) is used to determine oxygen concentrations in biological systems¹¹ and in biological labeling applications¹² and to investigate intracellular delivery of bioactive molecules.¹³ Excimer fluorescence between two or more pyrene molecules is used to detect various substrates,¹⁴

such as toxic metals in water,^{14e} glucose,¹⁵ and even explosives.¹⁶ In pyrene-based organic light-emitting diode (OLED) devices,¹⁷ bulky substituents are required to hinder excimer emission and $\pi-\pi$ stacking interactions, which have a quenching effect.¹⁸ Specific examples of OLEDs in which pyrene derivatives have been tuned to emit over the full visible color range incorporate 1,6-bis[*N*-phenyl-*N*-(*p*-R-phenyl)amino]pyrenes (R = CN, F, H, Me, ^tBu, OMe, NPh₂, NMePh),^{17g} tetrasubstituted pyrenes with bithiophene, phenylene, thienothiophene, or benzothiadiazole–thiophene units,^{17h} and the compounds pyrene-1-B(Mes)₂ (21) and 1,6-{B(Mes)₂}₂pyrene (Mes = 2,4,6-Me₃C₆H₃).^{17f} Substitution of pyrene at the 1-position with strong donor/acceptor-containing arylethynyl groups shows that it can behave as both an acceptor and a donor,¹⁹ whereas tetrasubstitution at the 1-, 3-, 6-, and 8-positions

Received: January 24, 2011

Published: July 13, 2011

with various arylolethynyl groups²⁰ and the formation of pyrene ethynylene oligomers²¹ leads to emission across the visible region. Mono-, bis-, tris-, and tetrakis(arylolethynyl)-substituted pyrenes have also been investigated for two-photon absorption (TPA),²² with the compound 1,3,6,8-tetrakis[[4-(*N,N*-dimethylamino)-phenyl]ethynyl]pyrene having a sizable TPA cross section of 1150 GM, much larger than those of the mono, bis, or tris derivatives.

All of the above pyrene derivatives involve substitution at the 1- or 1-, 3-, 6-, and 8-carbon atoms, the sites of maximum contributions of the HOMO and hence electrophilic aromatic substitution. Substituting pyrene at the 2- and 2,7-positions is synthetically challenging because of the presence of the nodal plane in the HOMO and LUMO (Figure 1), which lies perpendicular to the molecule and passes through the 2- and 7-positions.

As a result, very few photophysical and computational studies have been carried out on 2- and 2,7-substituted pyrenes. However, a few examples do exist. We reported that the iridium-catalyzed borylation of pyrene takes place exclusively at the 2- and 7-positions, yielding 2-(Bpin)pyrene (**2**) or 2,7-bis-(Bpin)pyrene (**9**) depending on the reaction conditions.^{1a} The cross coupling between **2** and a uridine base under harsh conditions and with long reaction times was subsequently reported to give a pyrene-modified nucleotide.²³ Calculations and photophysical studies showed that this derivative retained the optical properties of pyrene (weak electronic interaction between pyrene and the nucleotide). In contrast, the isomeric 1-pyrenyluridine was found to exhibit a strong electronic interaction between the pyrene moiety and the uridine π -system.²³ In the study of electron transfer in DNA, the absence of spectral signals due to π orbital conjugation with the uridine in the 2-substituted system leads to more straightforward spectra, from which it is easier to assign the electron transfer dynamics. A comparison of the effects of substitution of 1-, 2-, and 4-ethynylpyrenes (synthesized from tetrahydropyrene) onto uridine^{24a} or DNA modified by (2- or 4-iodophenyl)methylglycerol^{24b} has shown that the position of substitution has an effect on the photophysical properties of the compounds. For example, an absorption maximum of 357 nm for the 1-substituted compound is observed and compares to 336 nm for the 2-substituted compound. However, detailed studies of the effects of different substituents on the excited states or a comparison with pyrene for 2- and 2,7-derivatives are lacking. After this paper was submitted, the synthesis (from **9**) and crystal structures of four 2,7-bis(aryl)pyrenes (aryl = Ph, 2-thienyl, 2-(5-hexylthienyl), 2-thiazolyl) were reported, and their photophysical properties (vide infra) and behavior as p-type semiconductors in organic field-effect transistors (OFETs) were described.²⁵

In our companion paper,^{1b} we describe the facile synthesis of a library of 2- and 2,7-substituted pyrene compounds derived from **2** and **9**. In the current paper, we report the effects of the nature and position of substituents upon the photophysical properties of the compounds. We also report time-dependent density functional theory (TD-DFT)²⁶ calculations, through which a comparison of the B3LYP^{27–30} and CAM-B3LYP³¹ functionals is addressed. Indeed, it is known to be a challenge to obtain the correct ordering of states via TD-DFT calculations on pyrene itself.³²

We originally chose to investigate these compounds (Table 1) because they have potential for further application. The dimethylboron (B(Mes)₂) moiety (**7**, **8**, **13**, **20**, **21**) behaves as an efficient π -acceptor^{33–35} and is of interest in work involving



Figure 1. HOMO (bottom) and LUMO (top) of pyrene (B3LYP).

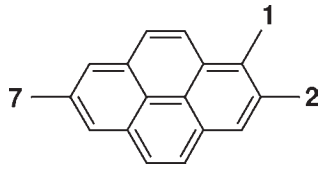
π -conjugated organic compounds containing 3-coordinate boron centers which have found applications in OLEDs, sensors, solar cells, and other materials.³³ Also, **16** (R = N(Ph)-C₆H₄-4-OMe)^{1c} is related to *N,N,N',N'*-tetraaryl-1,1'-biphenyl-4,4'-diamines (TPDs), in which there is a biphenyl moiety instead of a pyrene. These compounds are an important class of hole transporters in OLED devices.³⁶ Investigation into the effects of extending the conjugation length of pyrene by substitution at the 2- and 2,7-positions with arylolethynyl moieties will be of interest, as it is known that conjugated systems involving substitution of various arylolethynyl moieties onto a central core molecule, such as benzene,³⁷ anthracene,³⁸ and heterocyclopentadienes,³⁹ show interesting structural, electronic, and luminescent properties. Borylated arene compounds synthesized by iridium-catalyzed C–H borylation are important precursors to a range of derivatives.⁴⁰ To help understand the electronic influence of the Bpin moiety on aromatic systems, we investigated the photophysical properties of **2**, **9**, and **18**. The fluorescence lifetimes of **1** (R = C₃H₆CO₂H) and **3** (R = OC₃H₆CO₂H) are compared to that of the aforementioned fluorescence probe 4-(pyren-1-yl)butyric acid (**17**), which is used because of its long fluorescence lifetime (τ_f = 460 ns in MeOH).

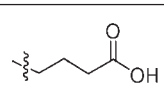
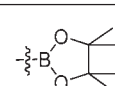
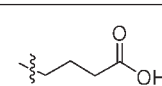
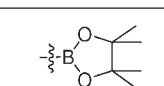
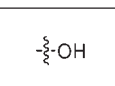
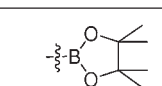
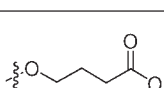
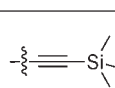
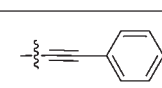
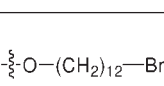
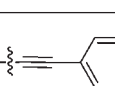
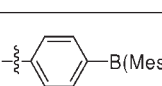
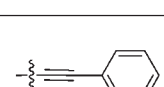
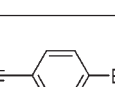
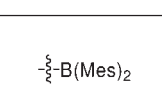
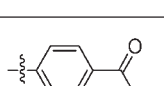
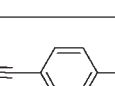
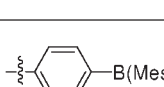
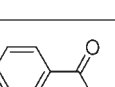
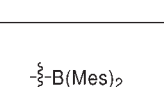
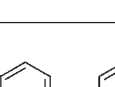
RESULTS AND DISCUSSION

Unsubstituted Pyrene. Before discussing the effects of substitution on pyrene, we first consider the photophysical properties of unsubstituted pyrene. As a monomer in cyclohexane solution, the absorption spectrum of pyrene consists of four bands (Figure 2): a weak band ($S_1 \leftarrow S_0$) at 372 nm (ϵ = 510 mol⁻¹ cm⁻¹ L) with vibrational fine structure, two bands ($S_2 \leftarrow S_0$ and $S_3 \leftarrow S_0$) at 334 and 272 nm, respectively, with regular vibrational structure (ϵ = 55000 and 54000 mol⁻¹ cm⁻¹ L, respectively), and a strongly allowed band ($S_4 \leftarrow S_0$) at 243 nm (ϵ = 88000 mol⁻¹ cm⁻¹ L).⁴¹ These transitions (Table 2) are referred to by a number of different nomenclatures, including those introduced by Clar⁴² and Platt⁴³ as well as those derived from the symmetry of the orbitals involved in the transitions.

Theory and linear dichroism studies^{10a,c,44} show that the $S_1 \leftarrow S_0$ and $S_3 \leftarrow S_0$ transitions are polarized along the short *y*-axis of pyrene while the $S_2 \leftarrow S_0$ and $S_4 \leftarrow S_0$ transitions are

Table 1. 2-, 2,7-, and 1-Substituted Pyrene Derivatives Studied in This Investigation



	2-R-pyrenes		2,7-R ₂ pyrenes		1-R-pyrenes
1		9 ^a		17	
2 ^a		10		18 ^a	
3		11		19	
4 ^b		12		20	
5		13		21	
6		14			
7		15 ^c			
8		16			

^a The methyl groups were replaced with hydrogens for TD-DFT calculations. ^b Calculations not performed on compound 4. ^c The C₈H₁₇ group was replaced with CH₃ for TD-DFT calculations.

polarized along the long z-axis (for the coordinate system, see Figure 3).

After excitation to higher excited states, transient absorption spectroscopy has shown the buildup of the S₁ population to be complete within 2 ps, with a wavelength-dependent time constant of 300–400 fs.⁴⁵ Fluorescence from the S₁ state is observed in the emission spectrum at 372 nm (in toluene) displaying resolved vibronic fine structure. The excited singlet state is exceptionally long-lived, with a fluorescence lifetime of 354 ns in degassed solution.^{41d} Low rate constants of fluorescence, $k_F = 10^6 \text{ s}^{-1}$, and intersystem crossing, $k_{ST} = 10^5 \text{ s}^{-1}$,^{41b} along with an uncompetitive rate of internal conversion, typical of rigid aromatic molecules, give rise to a significant fluorescence quantum yield of 0.64, with the remainder of excited singlet states undergoing intersystem crossing to a triplet state. Pyrene is widely known for its ability to form excimers in solution at concentrations

above ca. $10^{-5} \text{ mol dm}^{-3}$, giving rise to a broad, structureless emission band centered at 480 nm, while the intensity of emission due to the monomer decreases with increasing concentration.⁴¹

The energies of the S_n ← S₀ excitations in pyrene have also been the subject of many theoretical studies,³² ranging from early Pariser–Parr–Pople³²ⁱ calculations (where the importance of substituent position was recognized; molecules 5, 12, and 19 were explicitly considered) to TD-DFT and sophisticated wave function approaches.^{32h} Vertical excitation energies of pyrene obtained from TD-DFT calculations using the commonplace B3LYP exchange-correlation functional were reported by Parac and Grimme.^{32c} Comparison of these values with experimental band maxima (recorded in nonpolar solvents) shows that B3LYP accurately reproduces the S₂ ← S₀ excitation energy, but overestimates the S₁ ← S₀ energy, such that the order of the two states is incorrect. The approach used by Parac and Grimme, in which

they compare theoretically determined vertical excitation energies to band maxima in the absorption spectrum, is routinely used but is an approximation. The vertical excitation energy is the difference between the ground- and excited-state potential energy surfaces at the same geometry. For absorption energies, the appropriate geometry is the ground-state minimum. The error in this approximation was quantified by Dierksen and Grimme^{32f} by explicitly calculating the vibronic structure in the absorption spectrum using B3LYP with the Franck-Condon–Herzberg-Teller approximation. For the $S_2 \leftarrow S_0$ excitation, they noted that the B3LYP vertical excitation energy is 0.26 eV above the calculated $S_2^0 \leftarrow S_0^0$ (0, 0) transition energy. However, the value of the calculated (0, 0) transition energy was found to be 0.42 eV below the corresponding experimental (0, 0) value; this was attributed to a systematic underestimation of the excitation energies for states with ionic components in the wave function (in the valence bond picture)^{32d} when using TD-DFT with B3LYP. Therefore, the accurate reproduction^{32c} of the $S_2 \leftarrow S_0$ excitation energy using B3LYP is largely a result of the cancellation of these two factors; i.e., the excited-state curve is too low in energy, but this is offset by calculating the vertical energy rather than the (0, 0) transition energy. For the weakly allowed $S_1 \leftarrow S_0$ excitation, the vertical excitation energy was found to be 0.19 eV above the calculated $S_1^0 \leftarrow S_0^0$ (0, 0) transition energy. Unlike the $S_2 \leftarrow S_0$ excitation, the (0, 0) transition energy for the $S_1 \leftarrow S_0$ excitation was found to be 0.2 eV above the corresponding experimental (0, 0) value. As a result, there is no cancellation of the errors in this calculation and the $S_1 \leftarrow S_0$ excitation with B3LYP lies well above the (0, 0) transition energy observed experimentally. These B3LYP results suggest that an accurate DFT functional should yield vertical excitation energies that are higher in energy than the experimental (0, 0) values by

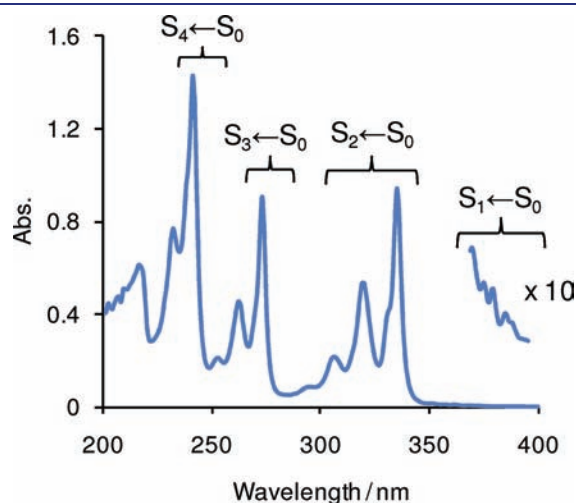


Figure 2. Absorption spectrum of pyrene (recorded in cyclohexane) with transitions labeled.

approximately 0.26 and 0.19 eV, thus giving wavelengths of 316 and 343 nm for the $S_2 \leftarrow S_0$ and $S_1 \leftarrow S_0$ excitations, respectively.^{32f}

We have calculated vertical excitation energies for pyrene using both B3LYP and CAM-B3LYP Coulomb-attenuated functionals.^{31,46} The former contains 20% exact exchange at all interelectron distances, while the latter includes 19% exact exchange at short interelectron distances, increasing smoothly to a limiting value of 65% as the interelectron distance increases. Coulomb-attenuated exchange-correlation functionals,⁴⁶ such as CAM-B3LYP,³¹ have recently been shown to improve the accuracy of ionic states in TD-DFT calculations on polycyclic aromatic hydrocarbons⁴⁷ and are attracting significant interest in the chemical literature. Our B3LYP vertical excitation energies for pyrene are consistent with those of Grimme and Parac.^{32c} The $S_2 \leftarrow S_0$ excitation is predicted to be at 340 nm with an oscillator strength of 0.25; the $S_1 \leftarrow S_0$ excitation is at 333 nm, with an oscillator strength of only 3×10^{-4} . These wavelengths can be compared with our aforementioned estimates of 316 and 343 nm, highlighting the incorrect order of states obtained using B3LYP. Using CAM-B3LYP, the order of the first and second excited states is the reverse of that found with B3LYP, so the experimental order is recovered. A similar observation was made for the ordering of states in naphthalene.⁴⁷ The $S_2 \leftarrow S_0$ excitation is now predicted to lie at 315 nm, with an oscillator strength of 0.31, which is in good agreement with our estimated theoretical value of 316 nm. However, the $S_1 \leftarrow S_0$ excitation is at 316 nm, with an oscillator strength of 2×10^{-4} , which is notably higher in energy than our estimated theoretical value of 343 nm, meaning the splitting is much too small. We note that the double-hybrid B2-PLYP functional also recovers the experimental order with a more accurate splitting.^{32j} These findings are fully consistent with previous studies using CAM-B3LYP, which illustrate that this functional often overestimates the energy of local excitations.⁴⁸ For both of these functionals, the $S_2 \leftarrow S_0$ excitation is primarily described by a HOMO \rightarrow LUMO transition and the $S_1 \leftarrow S_0$ excitation has approximately equal contributions of HOMO $- 1 \rightarrow$ LUMO and HOMO \rightarrow LUMO + 1 (Figure 4). It should be noted that, in TD-DFT, the vertical excitation energy is not, in general, equal to an orbital energy difference.

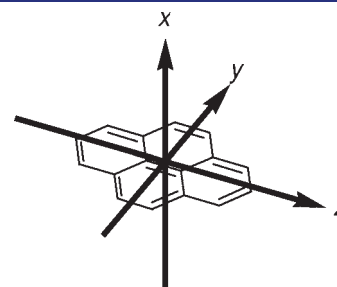


Figure 3. Principle Cartesian coordinate system used for pyrene.

Table 2. Summary of Terminology Used To Describe Optical Transitions in Pyrene^{41e}

transition	wavelength, nm (ϵ , mol ⁻¹ cm ⁻¹ L) ^a	symmetry	dominant configuration	polarization	Clar	Platt
$S_1 \leftarrow S_0$	372 (510)	B _{2u}	$b_{3u} \leftarrow b_{1g} - a_u \leftarrow b_{2g}$	y	α	L _b
$S_2 \leftarrow S_0$	334 (55000)	B _{1u}	$a_u \leftarrow b_{1g}$	z	p	L _a
$S_3 \leftarrow S_0$	272 (54000)	B _{2u}	$b_{3u} \leftarrow b_{1g} + a_u \leftarrow b_{2g}$	y	β	B _b
$S_4 \leftarrow S_0$	243 (88000)	B _{1u}	$b_{3u} \leftarrow b_{2g}$	z	β'	B _a

^a Recorded in cyclohexane.

Substituted Pyrenes. To compare the effects of substitution at the 1-, 2-, and 2,7-positions of pyrene, absorption, excitation, and emission spectra were recorded, and photoluminescence quantum yields and lifetimes were measured, for a series of derivatives. Spectroscopic data are given in Tables 3–5, selected spectra are presented in Figures 5–9, and absorption, emission, and excitation spectra for all compounds can be found in the Supporting Information. To avoid excimer formation, spectra were measured at low sample concentrations (10^{-5} – 10^{-6} mol dm $^{-3}$); therefore, our discussion refers to the behavior of pyrene monomers in solution. Tables listing the first five calculated singlet excitations for the

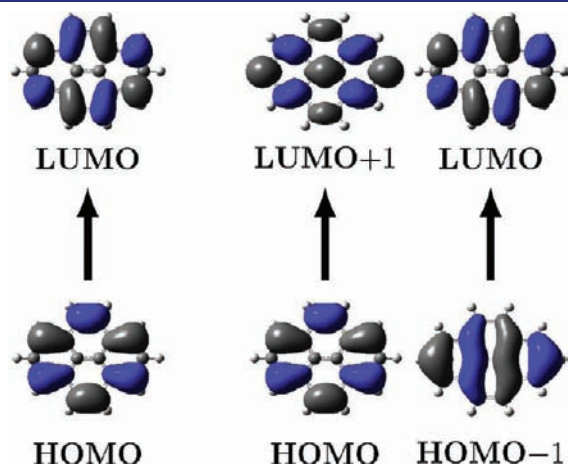


Figure 4. Dominant orbital contributions to the $S_2 \leftarrow S_0$ (left) and $S_1 \leftarrow S_0$ (right) excitations in pyrene (B3LYP).

molecules described are presented in the Supporting Information, and selected plots of key molecular orbitals contributing to the dominant transitions, along with a comparison of experimental and theoretical wavelengths, are shown in Figures 10–15.

Optical Properties. Donor and Acceptor Systems. First, the effects of attaching a series of donor and acceptor substituents to pyrene are discussed. The absorption spectra of 2-R-pyrenes {R = OC $_3$ H $_6$ CO $_2$ H (3), O(CH $_2$) $_{12}$ Br (4), C $_6$ H $_4$ -4-CO $_2$ Me (6), C $_6$ H $_4$ -4-B(Mes) $_2$ (7), B(Mes) $_2$ (8)} and 2,7-R $_2$ -pyrenes {R = OH (10), C $_6$ H $_4$ -4-CO $_2$ C $_8$ H $_{17}$ (15), N(Ph)-C $_6$ H $_4$ -4-OMe (16)} are similar to that of unsubstituted pyrene (Figure 2), and the $S_2 \leftarrow S_0$ excitation in these derivatives can be described as “pyrene-like”.⁴⁹ Despite the addition of strong acceptors 7 and 8 and donors 10 and 16 and increasing the conjugation length through phenyl substituents 6, 7, and 15, there is only a negligible bathochromic shift (0–7 nm) in the absorption maxima for the $S_2 \leftarrow S_0$ excitation (Figure 5). The vibrational progression is well resolved for compounds 3, 4, and 10 with a spacing of 1400 cm $^{-1}$. In the remaining compounds, the same vibrational progression is often observed, highlighting the pyrene-like nature of this excitation; however, the presence of overlapping higher energy electronic transitions often obscured some of the vibrational bands. Measured extinction coefficients for the “pyrene-like” $S_2 \leftarrow S_0$ excitation in 2- and 2,7-derivatives ($\epsilon = 54000$ – 143000 mol $^{-1}$ cm $^{-1}$ L) are, in most cases, larger than that for pyrene ($\epsilon = 69000$ mol $^{-1}$ cm $^{-1}$ L), with exceptionally high apparent values for R = C $_6$ H $_4$ -4-B(Mes) $_2$ (7), OH (10), and N(Ph)-C $_6$ H $_4$ -4-OMe (16) ($\epsilon = 143000$, 103000, and 112000 mol $^{-1}$ cm $^{-1}$ L, respectively). Closer examination of the spectra, especially for 7 and 16, clearly shows that another absorption overlaps with the pyrene-like one, contributing intensity and thus

Table 3. Spectroscopic Data for 2-Monosubstituted Pyrene Derivatives in Toluene Unless Otherwise Stated

R	$\lambda_{(S_1 \leftarrow S_0)}$, nm	ϵ , mol $^{-1}$ cm $^{-1}$ L	$\lambda_{(S_2 \leftarrow S_0)}$, nm	ϵ , mol $^{-1}$ cm $^{-1}$ L	λ_{em} , nm	ϕ_f^a	Stokes shift, cm $^{-1}$	τ_f^b , ns	τ_o^c , ns	
pyrene	362	600	338	69000	372	0.64	740	354	553	
1 ^d	C $_3$ H $_6$ CO $_2$ H	374	600	336	80000	374	0.52	0	622	1200
2	Bpin	385	1900	338	66000	386	0.72	70	82	114
3 ^d	OC $_3$ H $_6$ CO $_2$ H	382	5000	336	73000	382	0.77	0	59	77
4	O(CH $_2$) $_{12}$ Br	384	3800	340	54000	384	0.59	0	60	102
5	CCPh	390	1200	340	68000	399	0.44	600	71	161
6	C $_6$ H $_4$ -4-CO $_2$ Me	364	1100	341	66000	406	0.43	2800	74	172
7	C $_6$ H $_4$ -4-B(Mes) $_2$	378	2700	339	143000 ^e	414	0.47	2300	65	138
8	B(Mes) $_2$	413	2000	340	67000	434	0.68	1200	49	72

^a Fluorescence quantum yield measured in degassed solvent. ^b Fluorescence lifetime measured in degassed solvent. ^c Calculated from τ_f^b/ϕ_f^a . ^d Measured in MeOH. ^e Value enhanced due to the superposition with a broad low-energy absorption band (see the text).

Table 4. Spectroscopic Data for 2,7-Disubstituted Pyrene Derivatives in Toluene Unless Otherwise Stated

R	$\lambda_{(S_1 \leftarrow S_0)}$, nm	ϵ , mol $^{-1}$ cm $^{-1}$ L	$\lambda_{(S_2 \leftarrow S_0)}$, nm	ϵ , mol $^{-1}$ cm $^{-1}$ L	λ_{em} , nm	ϕ_f^a	Stokes shift, cm $^{-1}$	τ_f^b , ns	τ_o^c , ns	
pyrene	362	600	338	69000	372	0.64	740	354	553	
9	Bpin	398	5000	339	85000	400	0.88	250	36	41
10 ^d	OH	381	7000	338	103000 ^e	405	0.93	430	29	31
11	C \equiv C(TMS)	407	1600	337	51000	407	0.19	0	99	521
12	C \equiv CPh	410	3900	332	117000 ^e	418	0.29	460	16	55
13	C \equiv C-C $_6$ H $_4$ -4-B(Mes) $_2$	414	2800	344	120000 ^e	426	0.46	680	58	126
14	C \equiv C-C $_6$ H $_4$ -4-NMe $_2$	421	3300	343	136000 ^e	436	0.39	800	60	154
15	C $_6$ H $_4$ -4-CO $_2$ C $_8$ H $_{17}$	404	1500	340	69000	421	0.33	1000	49	148
16	N(Ph)-C $_6$ H $_4$ -4-OMe	453	2600	345	112000 ^e	482	0.30	1300	18	60

^a Fluorescence quantum yield measured in degassed solvent. ^b Fluorescence lifetime measured in degassed solvent. ^c Calculated from τ_f^b/ϕ_f^a . ^d Measured in MeOH. ^e Value enhanced due to the superposition with a broad low-energy absorption band (see the text).

Table 5. Spectroscopic Data for 1-Monosubstituted Pyrene Derivatives in Toluene Unless Otherwise Stated

R	$\lambda_{(S_1 \leftarrow S_0)}$, nm	ϵ , mol ⁻¹ cm ⁻¹ L	$\lambda_{(S_2 \leftarrow S_0)}$, nm	ϵ , mol ⁻¹ cm ⁻¹ L	λ_{em} , nm	ϕ_f^a	Stokes shift, cm ⁻¹	τ_f^b , ns	τ_o^c , ns
pyrene	362	600	338	69000	372	0.64	740	354	553
17 ^d	C ₃ H ₆ CO ₂ H	1700	342	68000	375	0.68	0	460	680
18	Bpin	7000	352	81000	379	0.81	70	35	43
19	C≡CPh	59000	362 ^e		391	0.61	2000	3	5
20	C ₆ H ₄ -4-B(Mes) ₂	54000	355 ^e		431	0.61	5000	2	3
21	B(Mes) ₂	54000	399 ^e		423	0.71	1400	3	4

^a Fluorescence quantum yield measured in degassed solvent. ^b Fluorescence lifetime measured in degassed solvent. ^c Calculated from τ_f^b/ϕ_f^a . ^d Measured in MeOH. ^e Not possible to assign separate S₂ ← S₀ and S₁ ← S₀ absorptions.

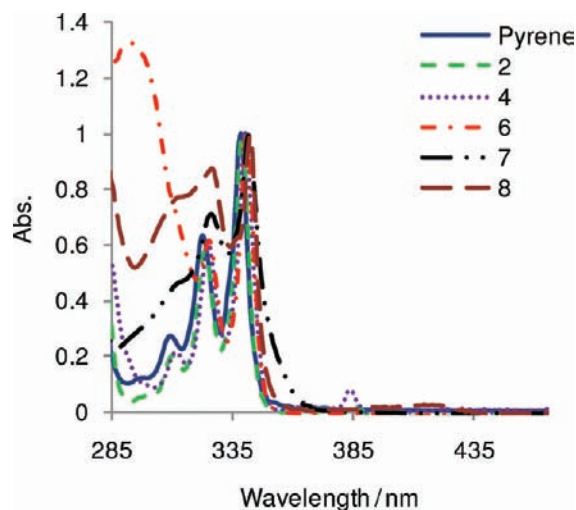


Figure 5. Absorption spectra of selected 2-monosubstituted pyrene systems showing the negligible bathochromic shift in the S₂ ← S₀ transition compared to that of pyrene.

leading to the anomalously large apparent ϵ values. In contrast, the S₁ ← S₀ excitation in pyrene is shown to be strongly affected by substitution at the 2- and 2,7-positions; hence, this excitation is “substituent-influenced”.⁵⁰ Bathochromic shifts of up to 90 nm in the S₁ ← S₀ excitation maxima are observed, and the excitation becomes much more allowed: their extinction coefficients generally increase in magnitude. The most allowed S₁ ← S₀ excitations occur for the oxygen-substituted compounds 3, 4, and 10 ($\epsilon = 3800\text{--}7000$ mol⁻¹ cm⁻¹ L, compared to $\epsilon = 600$ mol⁻¹ cm⁻¹ L for pyrene).

The absorption spectra of 1-R-pyrenes (R = C₆H₄-4-B(Mes)₂ (20), B(Mes)₂ (21)) display large differences when compared to those of pyrene and the 2- and 2,7-derivatives. Instead of clearly defined excitations, a broad absorption band with no vibrational progression is observed (Figure 6). Straightforward assignment of the separate S₂ ← S₀ and S₁ ← S₀ excitations is no longer possible. There is only one discernible maximum in this band, which is bathochromically shifted from the S₂ ← S₀ excitation maximum in pyrene and is strongly allowed with $\epsilon = 54000$ mol⁻¹ cm⁻¹ L. In the 1-substituted derivatives, substitution has a strong influence on both the S₂ ← S₀ and S₁ ← S₀ excitations.

Evidence for a substituent influence on the S₁ ← S₀ excitation is further observed in the emission spectra, which involve the reverse, i.e., S₀ ← S₁, transition (Figures 7 and 8). All compounds (regardless of substitution position) display a bathochromic shift from pyrene in their emission maxima, ranging from 10 to 110 nm.

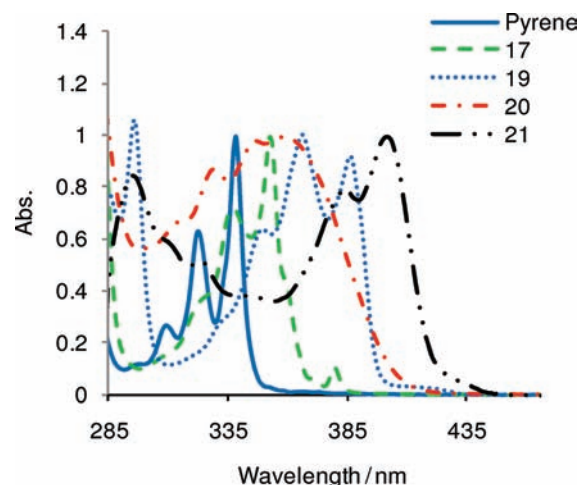


Figure 6. Absorption spectra of selected 1-monosubstituted pyrene systems showing the large bathochromic shift in the absorption maxima compared to that of pyrene.

The structure of the emission band of 3 (R = OC₃H₆CO₂H) and 4 (R = O(CH₂)₁₂Br) is similar to that of pyrene, displaying fine vibrational structure, whereas on moving to strong donors 10 and 16 or acceptors 7, 8, 20, and 21 the band broadens and all fine structure is lost. Stokes shifts are sizable for the esters 6 and 15, B(Mes)₂ derivatives 7, 8, 20, and 21, and N(Ph)-C₆H₄-4-OMe derivative 16, ranging from 1000 to 5000 cm⁻¹, suggesting that the excited-state electronic structure and geometry are somewhat different from those of the ground state. Fluorescence lifetimes were found to be much shorter for all of the above compounds than that of pyrene ($\tau_f = 354$ ns), consistent with the larger extinction coefficients observed and oscillator strengths (vide infra) for the S₁ ← S₀ excitation. Upon substitution at the 2- and 2,7-positions, the lifetimes are in the range of 18–74 ns, which are ca. 1–2 orders of magnitude longer than for the 1-substituted derivatives, for which $\tau_f = 2\text{--}3$ ns. It would appear that the effects on the allowedness of the S₁ ← S₀ transition are much more pronounced for 1-substituted derivatives than those substituted at the 2- and 2,7-positions, as evidenced by their shorter emission lifetimes. This observation is supported by comparing 16 with the known 1,6-isomer 1,6-bis[N-phenyl-N-(4-methoxyphenyl)amino]-pyrene,^{17g} the latter having a shorter fluorescence lifetime ($\tau_f = 9$ ns) compared to 16 ($\tau_f = 18$ ns). Quantum yields for the above compounds are in the range of 0.3–0.93 and are generally smaller when the substituent is a phenyl derivative (6, 7, 15, 20). Thus, values of 0.33 and 0.30 were measured for 15 and 16, respectively. It is worth comparing these with the value of 0.006

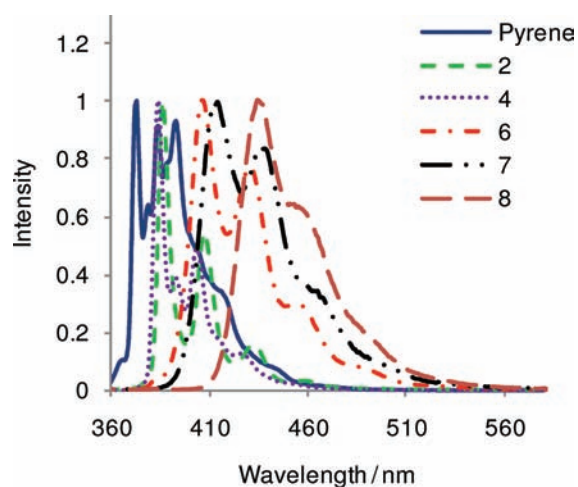


Figure 7. Emission spectra of selected 2-monosubstituted pyrene systems.

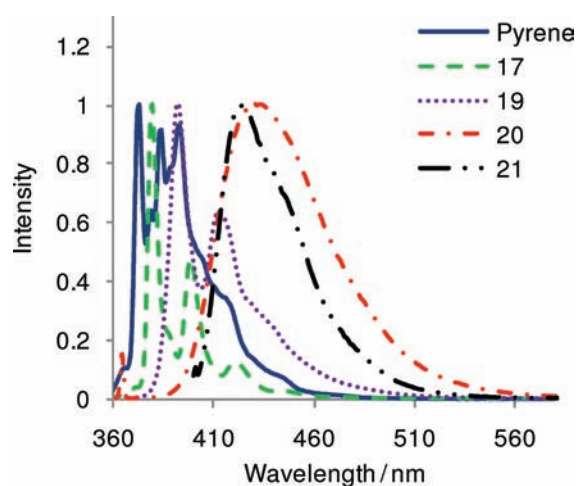


Figure 8. Emission spectra of selected 1-monosubstituted pyrene systems, with loss of vibrational resolution for compounds **20** ($R = C_6H_4-4-B(Mes)_2$) and **21** ($R = B(Mes)_2$).

reported²⁵ for 2,7-bis(phenyl)pyrene, perhaps reflecting the importance of thoroughly degassing samples to remove oxygen which can quench the emission due to the unusually long excited-state lifetimes of the 2- and 2,7-derivatives. Our ϕ_f value for **21** in toluene (0.71) differs from that recorded previously^{17f} in CH_2Cl_2 (~ 1.0). However, our absorption and emission spectra in toluene were in good agreement with those of Wang et al.^{17f}

Ethynyl Systems. Next we consider the effects of extending the conjugation length of pyrene with ethynyl substituents. Analogous to the donor and acceptor derivatives, a pyrene-like $S_2 \leftarrow S_0$ excitation is observed in the absorption spectra. Despite the extended conjugation in compounds 2-(C \equiv CPh)pyrene (**5**) and 2,7-bis(C \equiv CPh)pyrene (**12**), the $S_2 \leftarrow S_0$ absorption maxima undergo negligible shifts compared to that of unsubstituted pyrene. As well as these maxima, the absorption spectra also display a series of higher energy bands that are not well resolved. Similar behavior is observed in the related 1,4-bis(phenylethynyl)benzene, where broadening at high energies due to the rotation of the phenyl rings with respect to one another is observed.⁵¹ The increase in conjugation length has an influence on the $S_1 \leftarrow S_0$ excitation, which undergoes a 30–50 nm

bathochromic shift and becomes significantly more allowed ($\epsilon = 1200$ (**5**) and 3900 (**12**) $mol^{-1} cm^{-1} L$, compared to $\epsilon = 600$ $mol^{-1} cm^{-1} L$ for pyrene), again highlighting the substituent-influenced nature of this transition. Consistent with the strong influence on both the $S_2 \leftarrow S_0$ and $S_1 \leftarrow S_0$ excitations observed for the aforementioned 1-substituted derivatives, the absorption spectrum of the related 1-(C \equiv CPh)pyrene (**19**) shows a broad band with no clearly defined $S_2 \leftarrow S_0$ and $S_1 \leftarrow S_0$ excitations; however, unlike **20** and **21**, vibrational progression is observed with a spacing of 1400 cm^{-1} . This band has a maximum that is bathochromically shifted by 24 nm from the $S_2 \leftarrow S_0$ excitation in pyrene and is strongly allowed ($\epsilon = 59000$ $mol^{-1} cm^{-1} L$). Emission spectra of the three phenylethynyl derivatives **5**, **12**, and **19** are almost identical. The Stokes shift for **19** (2000 cm^{-1}) is much larger than those for **5** and **12** (600 and 460 cm^{-1} , respectively). Quantum yields are somewhat lower for the 2- and 2,7-derivatives, with the lowest value of $\phi_f = 0.29$ for **12** presumably due to the extra deactivation pathways from the excited state, caused by the additional phenylethynyl moiety. Analogous to the above donor/acceptor compounds, which showed that the influence on the allowedness of the $S_1 \leftarrow S_0$ transition is greatest when substitution is at the 1-position, the fluorescence lifetime of the 1-substituted derivative **19** ($\tau_f = 3$ ns) is much shorter than those of **5** and **12** ($\tau_f = 71$ and 16 ns, respectively).

The effects of altering the nature of the arylethynyl moiety on 2,7-bis(C \equiv CPh)pyrene (**12**) with a strong acceptor ($B(Mes)_2$, **13**) or a strong donor (NMe_2 , **14**) in the *para*-position are now considered. Similar to other 2- and 2,7-pyrene derivatives, pyrene-like $S_2 \leftarrow S_0$ excitation maxima are observed which are similar in energy to that of pyrene. Unlike **12**, the vibrational progression is better resolved and it is possible to measure a vibrational level spacing of 1500 – 1600 cm^{-1} (cf. 1500 cm^{-1} for pyrene; see the Supporting Information for vibrational level spacing values). However, the absorption spectra of these compounds are dominated by a broad, featureless band at lower energy than the pyrene-like transition (Figure 9). In **12**, the band appears as a small shoulder, but in **13** and **14**, the band broadens significantly, presumably due to essentially free rotation of the acceptor or donor arylethynyl moieties with respect to that of the pyrene core⁵¹ and indicative of extensive delocalization over the entire molecule. The apparent extinction coefficients for the pyrene-like $S_2 \leftarrow S_0$ absorption for all three compounds are exceptionally large ($\epsilon = 117000$ (**12**), 120000 (**13**), and 136000 (**14**) $mol^{-1} cm^{-1} L$), highlighting a strongly allowed process. However, these values likely represent the superposition of the pyrene-like absorption with that of at least one other broad lower-lying charge transfer type absorption (vide infra). In line with the other 2- and 2,7-derivatives, the $S_1 \leftarrow S_0$ excitation is substituent-influenced and, compared to pyrene, undergoes a bathochromic shift of 48–59 nm. All three compounds have similar $S_1 \leftarrow S_0$ extinction coefficients (2800 – 3900 $mol^{-1} cm^{-1} L$), which are much larger than that for pyrene. Despite the similarity of these extinction coefficients, the pure radiative lifetimes differ; the addition of a strong acceptor, **13** ($\tau_o = 126$ ns), or donor, **14** ($\tau_o = 154$ ns), increases the lifetime by a factor of 3 (**12**, $\tau_o = 55$ ns).

However, the fluorescence lifetime can be further increased when the aryl group is replaced with a trimethylsilyl (TMS) group. The compound 2,7-bis(C \equiv C(TMS))pyrene (**11**) has a lifetime of 99 ns and a quantum yield of 0.19; hence, its pure radiative lifetime is 521 ns, almost equivalent to that of pyrene, $\tau_o = 553$ ns. The effect of the TMS group is to reduce the

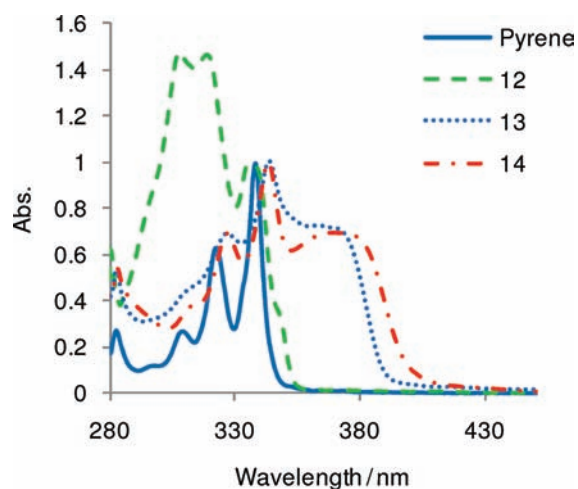


Figure 9. Absorption spectra of selected 2,7-bis-R-pyrene derivatives: R = C≡CPh (**12**), C≡C-C₆H₄-4-(BMe₂)₂ (**13**), and C≡C-C₆H₄-4-NMe₂ (**14**).

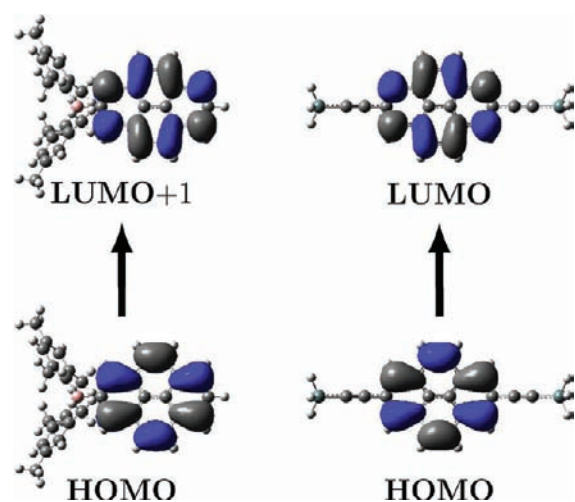


Figure 10. Pyrene-like transitions of compounds **8** and **11** (B3LYP).

conjugation length of the system and remove any rotational conformations associated with the phenyl group.^{38f} This appears to have the effect of increasing the fluorescence lifetime, despite its extinction coefficient for the S₁ ← S₀ transition ($\epsilon = 1600 \text{ mol}^{-1} \text{ cm}^{-1} \text{ L}$) being similar to those of the arylethynyl systems.

Bpin Derivatives. Substitution of pyrene with the Bpin moiety is now considered. The Bpin moiety is expected to be a modest π -acceptor and an inductive σ -donor. For 1-(Bpin)pyrene (**18**), separate S₂ ← S₀ and S₁ ← S₀ absorptions can now be resolved (cf. **19–21**, for which it was not possible to assign separate S₂ ← S₀ and S₁ ← S₀ excitations). Absorption spectra of 2-(Bpin)pyrene (**2**), 2,7-bis(Bpin)pyrene (**9**), and 1-(Bpin)pyrene (**18**) are very similar in overall appearance to that of pyrene; hence, the term pyrene-like for the S₂ ← S₀ excitation is very applicable. However, in the 1-substituted derivative **18**, there is a bathochromic shift in the absorption maximum of 14 nm, compared to negligible shifts for **2** and **9**. Furthermore, despite all three compounds showing well-resolved vibrational progressions of 1400 cm⁻¹, there is a slight broadening in the structure of the S₂ ← S₀ bands for **18**. Clearly, substitution at the 1-position exerts a greater influence on

the S₂ ← S₀ excitation than substitution at the 2- and 2,7-positions. Analogous to the above donor/acceptor/ethynyl compounds, the S₁ ← S₀ transition is substituent-influenced. The absorption has become more allowed, as reflected in the higher extinction coefficients ($\epsilon = 1900\text{--}7000 \text{ mol}^{-1} \text{ cm}^{-1} \text{ L}$, compared to $\epsilon = 600 \text{ mol}^{-1} \text{ cm}^{-1} \text{ L}$ for pyrene). Interestingly, the bathochromic shifts for the S₁ ← S₀ absorption are significantly larger for **2** and especially **9** than for **18**. Further effects are seen in the emission maxima, which undergo bathochromic shifts from pyrene (**2**, 14 nm; **9**, 28 nm; **18**, 7 nm), again being much larger for **2** and **9** than for **18**. The Stokes shifts are small, being 70–250 cm⁻¹, suggesting little change in the geometry between the ground and excited states. Quantum yields range from 0.72 to 0.88, all being higher than that of pyrene ($\phi_f = 0.64$), and fluorescence lifetimes are 4–10 times shorter than for pyrene, i.e., 35–82 ns compared to 354 ns. Interestingly, despite their different substitution positions, compounds **9** and **18** have almost identical lifetimes and quantum yields. Thus, Bpin derivatives show behavior similar to that of other pyrene derivatives (vide supra): substitution at the 2- and 2,7-positions has little influence on the S₂ ← S₀ absorption but a large influence on the S₁ ← S₀ absorption, whereas 1-substitution influences both the S₂ ← S₀ and S₁ ← S₀ absorptions. It is interesting to compare the monosubstituted derivatives 2-(Bpin)pyrene (**2**) and 2-(B(Mes)₂)pyrene (**8**). As expected from the fact that B(Mes)₂ is a stronger π -acceptor than Bpin,⁵² the bathochromic shifts of the S₁ ← S₀ absorption and emission maxima are much greater for **8** than for **2**, whereas again the S₂ ← S₀ absorptions for both are essentially invariant from that of pyrene. For the analogous 1-substituted derivatives 1-(Bpin)pyrene (**18**) and 1-(B(Mes)₂)pyrene (**21**), while it was not possible to assign separate S₂ ← S₀ and the S₁ ← S₀ absorptions for **21**, its emission maximum (423 nm) is considerably red-shifted from that of **18** (379 nm).

Butyric Acid Derivatives. Finally, we compare 4-(pyren-2-yl)-butyric acid (**1**) with commercially available 4-(pyren-1-yl)-butyric acid (**17**). For the purposes of this discussion, we classify the butyric acid moiety as a “noninteracting” substituent due to the absence of substantial conjugation, charge transfer, or inductive effects between the substituent and pyrene moiety. Absorption spectra of **1**, **17**, and pyrene are almost identical, with extinction coefficients for the S₂ ← S₀ excitation in the range of $\epsilon = 68000\text{--}80000 \text{ mol}^{-1} \text{ cm}^{-1} \text{ L}$. Hence, unlike other substituents at the 1-position (vide supra), the butyric acid group has a negligible influence on the S₂ ← S₀ excitation. The influence of substitution with butyric acid on the S₁ ← S₀ excitation is small, and both **1** and **17** have a negligible bathochromic shift in their emission maxima compared to that of pyrene. Stokes shifts for **1** and **17** are 0 cm⁻¹ compared to 740 cm⁻¹ for pyrene, suggesting almost no difference between the excited- and ground-state geometries. Quantum yields of 0.52–0.68 are again similar. However, the extinction coefficient for the S₁ ← S₀ excitation almost triples to $\epsilon = 1700 \text{ mol}^{-1} \text{ cm}^{-1} \text{ L}$ for **17** from $\epsilon = 600 \text{ mol}^{-1} \text{ cm}^{-1} \text{ L}$ for **1** and pyrene. This observation is further reflected in the fluorescence lifetimes, where τ_f is even longer for **1** (622 ns in MeOH) than for **17** (460 ns in MeOH), both being longer than that of pyrene (354 ns in toluene). Thus, we propose that **1** may be an even more efficient oxygen sensor in biological systems than **17** (vide supra),¹¹ and its unusually long fluorescence lifetime should make it amenable to use in time-resolved imaging applications.¹² Analogous to the other compounds investigated in this study, it is apparent that even when a noninteracting substituent is attached to pyrene, there is still an influence on the S₁ ← S₀ excitation regardless of the

substitution position. However, even in **1** and **17**, the influence on the $S_1 \leftarrow S_0$ absorption is much more pronounced when substitution occurs at the 1-position of pyrene, as seen by larger extinction coefficients and shorter fluorescence lifetimes, whereas when substituted at the 2-position, the influence on the $S_1 \leftarrow S_0$ excitation is much less and the molecule displays properties similar to those of unsubstituted pyrene.

TD-DFT Calculations. In relation to the above experimental observations, we now discuss the results of our TD-DFT calculations of vertical excitation energies. Initially, we focus on results obtained with the B3LYP functional, which has very recently been used to examine electronic transitions in four 2,7-bis(aryl)pyrenes.²⁵

Given the similarities in their behavior, we first consider the 2- and 2,7-substituted pyrene derivatives. As noted above (Figure 4), there is a nodal plane in the HOMO and LUMO of pyrene which lies perpendicular to the molecule and passes through the 2- and 7-positions. It is therefore unlikely that these orbitals will be significantly affected by substitution at these positions. However, the HOMO - 1 and LUMO + 1 orbitals have nonzero contributions at the 2- and 7-positions; therefore, substitution here is likely to influence the orbitals. The extent of this influence is dependent upon the nature of the substituent. An inspection of the calculated results for each 2- and 2,7-substituted compound shows that the majority do have an electronic transition which is directly comparable to the $S_2 \leftarrow S_0$ (HOMO \rightarrow LUMO) transition in pyrene; representative examples from compounds **8** and **11** are shown in Figure 10. It is important to stress that although the ordering of the orbitals might not be the same as seen in pyrene, it is the nature of the orbitals involved in the relevant transition that is of interest. For the majority of compounds, the $S_2 \leftarrow S_0$ transition involves the same orbitals as in the $S_2 \leftarrow S_0$ transition of unsubstituted pyrene. However, for compounds **1**, **7**, **12**, and **13** the analogous transition is the first, fourth, fourth, and fourteenth excitation, respectively (compounds **14**, **15**, and **16** had no identifiable transition which was comparable to the $S_2 \leftarrow S_0$ transition of pyrene in the low-lying excitations considered here). As the orbitals involved in this transition are unaffected by substitution, the energy of the transition should closely match that of the same transition in pyrene. All of the transitions are within 10 nm of the pyrene value, reproducing the small bathochromic shifts in the $S_2 \leftarrow S_0$ excitation maxima observed experimentally. As expected, the noninteracting effect of the butyric acid substituent in compound **1** is small enough that the results are virtually identical to those for pyrene (i.e., 341 nm for **1** vs 340 nm for pyrene), including the incorrect ordering of the first two states such that the strongly allowed HOMO \rightarrow LUMO transition is computed to be the lowest energy excitation.

The experimentally observed bathochromic shift for the $S_1 \leftarrow S_0$ transition upon substitution at the 2- and 2,7-positions is reproduced; the origin of this shift lies in the nature of the orbitals involved in the transition. The delocalization of the orbitals over the substituent for the HOMO - 1 and LUMO + 1 is shown for compound **11** in Figure 11 wherein they can be seen to extend over both the pyrene moiety and the (trimethylsilyl)ethynyl moiety. The effect of substitution can be seen by comparing these orbitals with those of unsubstituted pyrene in Figure 4. The DFT calculations have therefore successfully reproduced the experimental observation of the $S_1 \leftarrow S_0$ excitation being substituent-influenced. For some of the large substituents, the assignment of a transition which resembles the $S_1 \leftarrow S_0$ transition in pyrene is

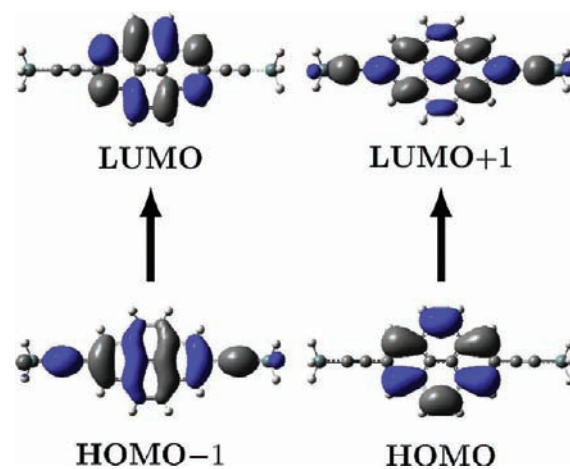


Figure 11. Dominant transitions of the $S_1 \leftarrow S_0$ excitation of compound **11** (B3LYP).

difficult as the orbitals delocalize to a much larger extent and the contribution from each orbital pair to the transition is no longer equal. This is seen in compounds such as **13** and **14** and may be the reason that the bathochromic shift is much larger here than in the other compounds.

We now consider DFT results for the 1-substituted pyrene derivatives. All four orbitals involved in the $S_2 \leftarrow S_0$ and $S_1 \leftarrow S_0$ excitations of pyrene have nonzero orbital contributions at the 1-position. Therefore, consistent with the shifts in wavelength, substitution at this position is expected to influence the orbitals. For all five 1-substituted compounds, the lowest energy state arises from a transition resembling the $S_2 \leftarrow S_0$ excitation of pyrene. The experimental results suggest that the $S_1 \leftarrow S_0$ transition becomes increasingly allowed when pyrene is substituted at the 1-position (cf. **17** and **18**). The theoretical results predict the first excitation to have a high oscillator strength; however, this transition is actually of the $S_2 \leftarrow S_0$ type seen in unsubstituted pyrene. In **18**, the bathochromic shift that was observed experimentally for this $S_2 \leftarrow S_0$ excitation maximum was reproduced, thus highlighting the greater influence of the Bpin substituent on the $S_2 \leftarrow S_0$ excitation when substituted at the 1-position. Given that it was difficult to distinguish separate $S_2 \leftarrow S_0$ and $S_1 \leftarrow S_0$ excitations experimentally for compounds **19**, **20**, and **21**, it is also difficult to draw any firm conclusions about the agreement between experimental and theoretical data for these compounds. As expected, our calculations on **19** show that the optimized geometry is planar, contrary to that reported elsewhere.¹⁹

The results obtained for the pyrene derivatives using CAM-B3LYP largely reflect the trends seen using B3LYP. Using CAM-B3LYP, transitions analogous to the $S_1 \leftarrow S_0$ excitation in pyrene are predicted to be the lowest energy ones for the 2- and 2,7-substituted compounds. All of the states that were unidentifiable or difficult to assign with B3LYP were more easily assigned with CAM-B3LYP. The results obtained using CAM-B3LYP for the 1-substituted derivatives also reflect those obtained using B3LYP, and the lowest energy transition for these derivatives was computed to be equivalent to the $S_2 \leftarrow S_0$ transition in pyrene. The plots in Figures 12 and 13 show a comparison of the wavelengths of those transitions which are directly comparable to the $S_1 \leftarrow S_0$ and $S_2 \leftarrow S_0$ transitions of pyrene in terms of orbitals involved, calculated using B3LYP and CAM-B3LYP,

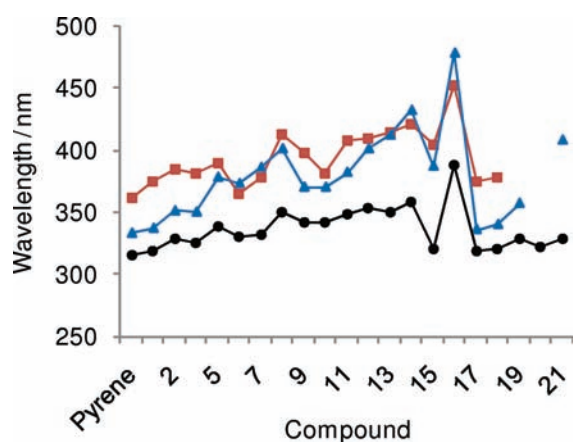


Figure 12. Comparison of theoretical and experimental wavelengths for the $S_1 \leftarrow S_0$ excitation in pyrene derivatives: squares, experiment; triangles, B3LYP; circles, CAM-B3LYP.

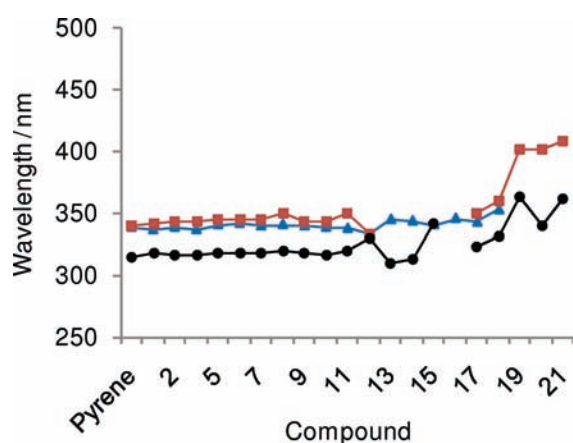


Figure 13. Comparison of theoretical and experimental wavelengths for the $S_2 \leftarrow S_0$ excitation in pyrene derivatives: squares, experiment; triangles, B3LYP; circles, CAM-B3LYP.

with those measured experimentally. It is clear that, for both transitions, theory is able to reproduce the general trend in wavelengths observed experimentally. To quantify this, wavelengths were uniformly shifted to the experimental value of pyrene and mean absolute errors were determined. For $S_1 \leftarrow S_0$, the B3LYP and CAM-B3LYP errors are 19 and 13 nm, respectively. For $S_2 \leftarrow S_0$, the errors are notably smaller, at just 4 nm for both functionals.

It is clear from the results that certain substituents have a much more significant effect than others. Compounds with the Bpin substituent show modest variation from the energies of the $S_1 \leftarrow S_0$ transition seen in unsubstituted pyrene. However, the effect of $B(\text{Mes})_2$ (compounds **8** and **21**), $C_6H_4-4-B(\text{Mes})_2$ (compounds **7** and **20**), and $C\equiv C-C_6H_4-4-B(\text{Mes})_2$ (compound **13**) is much larger. Given this, identification of the pyrene-like $S_1 \leftarrow S_0$ transition was difficult for these compounds. The roles of boron in these two types of substituents (Bpin/ $B(\text{Mes})_2$) are significantly different (vide supra). When bonded to the mesityl group, the empty p-orbital of boron facilitates extensive delocalization over the substituent. However, this effect is moderated by π -bonding with the oxygen atoms in the Bpin groups, and there is much less delocalization between boron and the pyrene

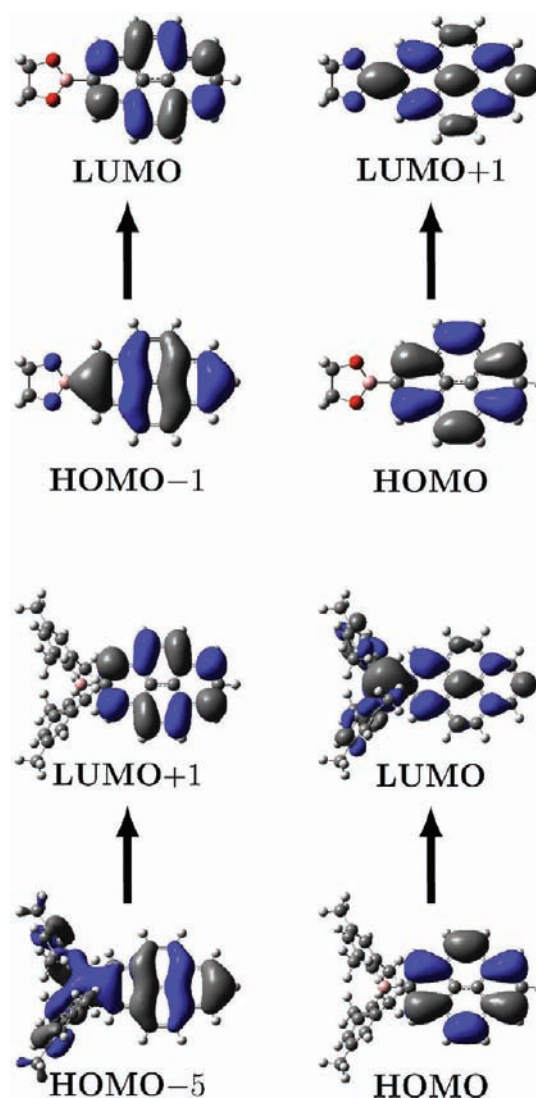


Figure 14. $S_1 \leftarrow S_0$ excitation for 2-R-pyrene derivatives **2** ($R = \text{Bpin}$, top) and **8** ($R = B(\text{Mes})_2$, bottom) highlighting the difference between the two boryl moieties (B3LYP).

π -system (Figure 14). Depending upon the nature of the substituent, pyrene is shown to behave as either an acceptor or a donor. Experimentally, donor substituents appear to have a greater influence on the $S_1 \leftarrow S_0$ transition. In **14** and **16**, the bathochromic shift in the absorption maxima and extinction coefficients for the $S_1 \leftarrow S_0$ transition are generally greater than for the acceptor-substituted derivatives **8**, **13**, and **15**. Hence, pyrene behaves more efficiently as an acceptor than as a donor in these compounds. These observations of bathochromic shifts are reproduced by our calculations. The HOMOs of **14** and **16** have notable contributions from the nitrogen atom, indicating that the low-lying transitions involve redistribution of charge from the nitrogen lone pair to the pyrene moiety. Conversely, the LUMOs of **8** and **13** involve the boron atom, and the $S_1 \leftarrow S_0$ transition for these compounds involves electron density moving from pyrene into the empty p-orbital of boron. As noted previously, for compounds **13** and **14** in particular, broad peaks observed in the absorption spectra overlap with the pyrene-like $S_2 \leftarrow S_0$ transition on the low-energy side. For **13**, the TD-DFT calculations (CAM-B3LYP) show a strongly allowed transition ($f = 3.39$)

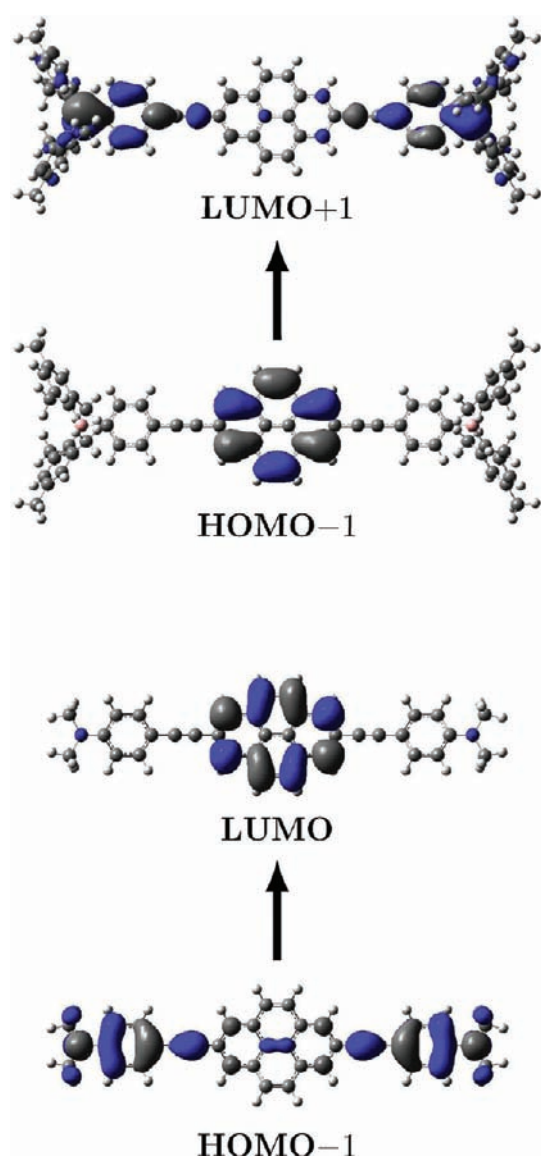


Figure 15. Low- Λ excitations: $S_6 \leftarrow S_0$ excitation in compound **13** (top) and $S_3 \leftarrow S_0$ excitation in compound **14** (bottom) (B3LYP).

involving $\text{HOMO} \rightarrow \text{LUMO}$ and $\text{HOMO} - 2 \rightarrow \text{LUMO} + 1$, only slightly higher in energy than the lowest energy transition for which $f = 0.003$ (see Table S3, Supporting Information). The intense absorption results from a delocalized state which generally involves charge transfer from the core toward the empty p-orbitals on the $\text{B}(\text{Mes})_2$ groups. For compound **14**, a related situation arises. This time, a strongly allowed transition ($f = 2.35$) involving $\text{HOMO} \rightarrow \text{LUMO} + 1$ and $\text{HOMO} - 1 \rightarrow \text{LUMO} + 2$ results in charge transfer from the nitrogen lone pairs toward the core of the molecule. Thus, for both the extended π -acceptor and π -donor conjugated systems, these charge transfer absorptions lie between the $S_1 \leftarrow S_0$ and pyrene-like $S_2 \leftarrow S_0$ absorptions.

We have previously demonstrated that B3LYP excitation energies are significantly underestimated when there is negligible overlap between the occupied and unoccupied orbitals involved in the excitation; we proposed a simple diagnostic quantity, Λ ,⁴⁷ to measure the overlap and predict such breakdown. Two of the substituted pyrenes exhibited low- Λ , charge transfer excitations, namely, compounds **13** and **14**. When calculated using B3LYP,

these excitations are the sixth (**13**) and third (**14**) excitations and should be expected to be significantly too low in energy. Using CAM-B3LYP, both excitations increase in energy to become at least the sixth excitation and have essentially zero oscillator strength, consistent with a low Λ value. Figure 15 illustrates the nature of these excitations for compounds **13** and **14**.

CONCLUSIONS

The photophysical properties of a range of 2- and 2,7-substituted pyrene derivatives and 1-substituted pyrenes were investigated using both experimental and TD-DFT studies. The TD-DFT calculations employed both the B3LYP and CAM-B3LYP functionals. Using CAM-B3LYP, the ordering of states in pyrene was correctly predicted. Both functionals were able to reproduce the general trends in wavelengths observed experimentally for the pyrene derivatives and provide insight into the experimental results through an analysis of orbital transitions.

It was shown that, upon changing the substitution position and the nature of the substituent on pyrene, stark differences were observed in the photophysical properties of the compounds. Generally, for the 2- and 2,7-derivatives, the $S_2 \leftarrow S_0$ excitation can be considered to be pyrene-like, as indicated by a very small bathochromic shift in its energy and retention of the vibrational progression. However, the $S_1 \leftarrow S_0$ excitation in these derivatives is found to be substituent-influenced, as indicated by large bathochromic shifts in its energy and an increase in allowedness reflected by higher extinction coefficients and shorter lifetimes. The $S_2 \leftarrow S_0$ excitation generally involves the HOMO and LUMO orbitals, which have nodes at the 2- and 7-positions. However, the $S_1 \leftarrow S_0$ excitation involves the $\text{HOMO} - 1$ and $\text{LUMO} + 1$ orbitals, which have nonzero contributions at the 2- and 7-positions; hence, the substituent influences this transition and the resulting emission considerably.

In contrast, substitution at the 1-position has a strong influence on both the $S_1 \leftarrow S_0$ and $S_2 \leftarrow S_0$ excitations. In the case of highly conjugated 1-substituted systems, it is not possible to distinguish between the two excitations in the experimental spectra. However, from the very short fluorescence lifetimes, it is apparent that the influence on the allowedness of the $S_1 \leftarrow S_0$ excitation is much stronger in the 1-substituted derivatives than in the 2- and 2,7-pyrenes. All of the orbitals involved in the $S_1 \leftarrow S_0$ and $S_2 \leftarrow S_0$ excitations have nonzero contributions at the 1-position, hence the significant influence on both transitions in the 1-substituted pyrene derivatives.

For all derivatives, modest (0.19) to high (0.93) fluorescence quantum yields were observed. For the 2- and 2,7-derivatives, fluorescence lifetimes exceeding 16 ns were measured, with most being ca. 50–80 ns. The 4-(pyren-2-yl)butyric acid derivative (**1**) has an exceptionally long fluorescence lifetime, 622 ns, significantly longer than that of the commercially available and widely employed 4-(pyren-1-yl)butyric acid (**17**), suggesting that it should be even more effective for measuring cellular oxygen concentrations or as a probe for time-resolved imaging of biosystems.

Overall, the results reported herein and in our forthcoming paper^{1b} show that 2- and 2,7-pyrene derivatives have a unique range of photophysical and structural properties that differ from those of the more “traditional” 1-substituted pyrene derivatives. These new derivatives, now available via straightforward, high-yielding synthetic routes, will be of interest in a wide range of

both existing and new applications, such as fluorescence probes and labels, OLED devices, and molecular sensors.

EXPERIMENTAL SECTION

General Information. The syntheses of the compounds are reported elsewhere,¹ except for **17**, which was purchased from Alfa Aesar. All photophysical measurements were carried out in HPLC-grade solvent. UV–vis absorption spectra and extinction coefficients were obtained on a Hewlett-Packard 8453 diode array spectrophotometer using standard 1 cm width quartz cells. Fluorescence spectra were recorded on a Horiba Jobin-Yvon Fluorolog FL 3-22 Tau spectrophotometer. For luminescence quantum yield and lifetime measurements, dilute solutions (10^{-5} – 10^{-6} M) of the compounds were frozen–thawed–degassed to remove any dissolved oxygen. Photoluminescence quantum yields were measured using an integrating sphere (Horiba Jobin-Yvon) following reported methods.⁵³ Luminescence lifetimes of less than 50 ns were recorded on a home-built time-correlated single-photon-counting (TCSPC) spectrometer. Samples were excited using either a pulsed laser diode (IBH NanoLED, 373 nm, 1 MHz pulse train, fwhm 100 ps) or the third harmonic of a cavity-dumped, mode-locked Ti–sapphire laser (Coherent MIRA-D, 300 nm, 4.5 MHz pulse train, fwhm <150 fs). Fluorescence from the sample was collected at 90° to the incident beam, and the emission wavelength was selected by a monochromator (Horiba Jobin-Yvon Triax-190) before detection using a single-photon avalanche diode (idQuantique id100-50). The signal derived from the detector was used as the start pulse for a time-to-amplitude converter, TAC (Ortec 567), operating in reverse-TAC mode. The stop pulse was derived from the cavity-dumper synchronization pulse or diode driver. The output of the TAC was measured using a pulse-height analyzer (Ortec Trump-8K) held in a PC. Instrument response functions for the two excitation sources, obtained using a Ludox scatterer, were 180 and 110 ps fwhm. Decays were analyzed by iterative deconvolution of the instrument response function with a sum of exponentials and nonlinear least-squares regression.⁵⁴ Goodness of fit was assessed by minimizing the reduced χ^2 function and a visual inspection of the weighted residuals. Each trace contained at least 10000 counts in the peak channel. When the lifetimes exceeded 50 ns, they were recorded by the determination of the decay in fluorescence intensity as a function of time following excitation. The samples were excited by the output of either a nitrogen laser (337 nm, fwhm < 5 ns) or the third harmonic of a Q-switched Nd:YAG laser (355 nm, fwhm < 5 ns). Fluorescence was collected at 90° to the incident beam, the emission wavelength was selected by a monochromator (Horiba Jobin-Yvon Triax-320), and the emission intensity was detected by a photomultiplier (Hamamatsu R928). Using 25 Ω termination, an instrument response function of <15 ns fwhm was obtained. The output of the photomultiplier tube was acquired using a digital storage oscilloscope (LeCroy WaveJet 324) and averaged over 265 laser shots before transfer to a PC and analysis (Excel).

TD-DFT Calculations. All calculations in the present study were carried out at B3LYP/6-31G*-optimized ground-state geometries. All excitation energies are singlet vertical excitations for isolated molecules, determined using the cc-pVTZ basis set, except for excitations of the largest compound **13**, which were performed using 6-31G*. Calculations were performed using both the B3LYP and CAM-B3LYP Coulomb-attenuated approximations. To assess the influence of solvent, additional B3LYP/6-31G* calculations on pyrene and molecules **13** and **14** were performed using a toluene solvent polarizable continuum model with dielectric constant $\epsilon = 2.379$. It is expected that these two molecules would experience the largest solvatochromic effects. The excitation energies decrease by no more than 0.1 eV. All calculations were carried out using the Gaussian 03⁵⁵ or Dalton⁵⁶ packages.

ASSOCIATED CONTENT

S Supporting Information. Absorption, emission, and excitation spectra, vibrational level spacing for the $S_2 \leftarrow S_0$ absorption, tables listing the first five calculated singlet excitations, and complete ref 55. This material is available free of charge via the Internet at <http://pubs.acs.org>.

AUTHOR INFORMATION

Corresponding Author

todd.marder@durham.ac.uk

ACKNOWLEDGMENT

A.G.C. and A.D.D. thank EPSRC for postgraduate studentships. Z.L. thanks the Royal Society and BP for a China Incoming Fellowship. A.S. thanks Marie-Curie (Grant EU-FP7) and DAAD for postdoctoral fellowships. T.B.M. thanks the Royal Society for a Wolfson Research Merit Award. We are grateful to Durham University for the provision of high-performance computing facilities.

REFERENCES

- (1) Compounds **2** and **9** were reported in the following: (a) Coventry, D. N.; Batsanov, A. S.; Goeta, A. E.; Howard, J. A. K.; Marder, T. B.; Perutz, R. N. *Chem. Commun.* **2005**, 2172–2174. (b) The application of these two compounds in the synthesis of the remaining 2- and 2,7-derivatives in the current paper will be reported shortly: Crawford, A. G.; Liu, Z.; Mkhaliid, I. A. I.; Thibault, M.-H.; Schwarz, N.; Alcaraz, G.; Steffen, A.; Collings, J. C.; Marder, T. B. Manuscript in preparation, presented in part at Pacificchem 2010, Symposium (No. 35) on Organoboron, Organosilicon and Organophosphorus as Optoelectronic and Energy Related Materials, Honolulu, Dec 17, 2010; ID No. 590. (c) A synthesis and partial characterization of **1** has been reported previously: Klassen, S. E.; Daub, G. H.; Vanderjagt, D. L. *J. Org. Chem.* **1983**, *48*, 4361–4366. (d) A synthesis of **10** has been reported previously: Boldt, P.; Bruhnke, D. *J. Prakt. Chem.* **1994**, *336*, 110–114. (e) Compound **16** has appeared in a patent: Seo, J. D.; Lee, K. H.; Kim, H. J.; Park, C. G.; Oh, H. Y. *Eur. Pat. Appl.* EP 1437395, 2004 (CAS no. 722499-18-5). (f) Compound **18** has been reported previously: Beinhoff, M.; Weigel, W.; Jurczok, M.; Rettig, W.; Modrakowski, C.; Brüdgam, I.; Hartl, H.; Schlüter, A. D. *Eur. J. Org. Chem.* **2001**, 3819–3829. (g) Compound **19** has been reported previously in ref 19. (h) A discussion regarding compound **21** can be found in ref 17f, vide infra.
- (2) (a) Netzelt, T. L.; Nafisi, K.; Headrick, J.; Eaton, B. E. *J. Phys. Chem.* **1995**, *99*, 17948–17955. (b) Huber, R.; Fiebig, T.; Wagenknecht, H.-A. *Chem. Commun.* **2003**, 1878–1879. (c) Trifonov, A.; Buchvarov, I.; Wagenknecht, H.-A.; Fiebig, T. *Chem. Phys. Lett.* **2005**, *409*, 277–280. (d) Kaden, P.; Mayer-Enthart, E.; Trifonov, A.; Fiebig, T.; Wagenknecht, H.-A. *Angew. Chem., Int. Ed.* **2005**, *44*, 1636–1639.
- (3) (a) Okamoto, A.; Tainaka, K.; Nishiza, K.-I.; Saito, I. *J. Am. Chem. Soc.* **2005**, *127*, 13128–13129. (b) Valis, L.; Mayer-Enthart, E.; Wagenknecht, H.-A. *Bioorg. Med. Chem. Lett.* **2006**, *16*, 3184–3187. (c) Malinovskii, V. L.; Häner, R. *Eur. J. Org. Chem.* **2006**, 3550–3553. (d) Seo, Y. J.; Rhee, H.; Joo, T.; Kim, B. H. *J. Am. Chem. Soc.* **2007**, *129*, 5244–5247.
- (4) (a) Malinovskii, V. L.; Samain, F.; Häner, R. *Angew. Chem., Int. Ed.* **2007**, *46*, 4464–4467. (b) Bittermann, H.; Siegemund, D.; Malinovskii, V. L.; Häner, R. *J. Am. Chem. Soc.* **2008**, *130*, 15285–15287.
- (5) (a) Nakamura, M.; Fukunaga, Y.; Sasa, K.; Ohtoshi, Y.; Kanaori, K.; Hayashi, H.; Nakano, H.; Yamana, K. *Nucleic Acids Res.* **2005**, *33*, 5887–5895. (b) Nakamura, M.; Ohtoshi, Y.; Yamana, K. *Chem. Commun.* **2005**, 5163–5165. (c) Nakamura, M.; Shimomura, Y.; Ohtoshi, Y.; Sasa, K.; Hayashi, H.; Nakano, H.; Yamana, K. *Org. Biomol. Chem.* **2007**, *5*, 1945–1951.

- (6) Kool, E. T.; Morales, J. C.; Guckian, K. M. *Angew. Chem., Int. Ed.* **2000**, *39*, 990–1009.
- (7) (a) Wilson, J. N.; Gao, J.; Kool, E. T. *Tetrahedron* **2007**, *63*, 3427–3433. (b) Mayer-Enthart, E.; Wagner, C.; Barbaric, J.; Wagenknecht, H.-A. *Tetrahedron* **2007**, *63*, 3434–3439. (c) Teo, Y. N.; Wilson, J. N.; Kool, E. T. *J. Am. Chem. Soc.* **2009**, *131*, 3923–3933. (d) Samain, F.; Ghosh, S.; Teo, Y. N.; Kool, E. T. *Angew. Chem., Int. Ed.* **2010**, *49*, 7025–7029.
- (8) Okamoto, A.; Kanatani, K.; Saito, I. *J. Am. Chem. Soc.* **2004**, *126*, 4820–4827.
- (9) Kashida, H.; Asanuma, H.; Komiyama, M. *Chem. Commun.* **2006**, 2768–2770.
- (10) (a) Kalyanasundaram, K.; Thomas, J. K. *J. Am. Chem. Soc.* **1977**, *99*, 2039–2044. (b) Kalyanasundaram, K. *Photochemistry in Microheterogeneous Systems*, Academic Press: Orlando, FL, 1987; pp 39–41. (c) Perry, M.; Carra, C.; Chrétien, M. N.; Scaiano, J. C. *J. Phys. Chem. A* **2007**, *111*, 4884–4889.
- (11) (a) Vaughan, W. M.; Weber, G. *Biochemistry* **1970**, *9*, 464–473. (b) Ribou, A.-C.; Vigo, J.; Salmon, J.-M. *Photochem. Photobiol.* **2004**, *80*, 274–280. (c) Berezin, M. Y.; Achilefu, S. *Chem. Rev.* **2010**, *110*, 2641–2684.
- (12) (a) Flamm, M.; Schachter, D. *Nature* **1982**, *298*, 290–292. (b) Fujimori, E.; Shambaugh, N. *Biochim. Biophys. Acta* **1983**, *742*, 155–161. (c) Lee, J. A.; Fortes, P. A. G. *Biochemistry* **1985**, *24*, 322–330. (d) Ebata, K.; Masuko, M.; Ohtani, H.; Kashiwasake-Jibu, M. *Photochem. Photobiol.* **1995**, *62*, 836–839. (e) Sugahara, D.; Amano, J.; Irimura, T. *Anal. Sci.* **2003**, *19*, 167–169.
- (13) (a) Takeuchi, T.; Kosuge, M.; Tadokoro, A.; Sugiura, Y.; Nishi, M.; Kawata, M.; Sakai, N.; Matile, S.; Futaki, S. *ACS Chem. Biol.* **2006**, *1*, 299–303. (b) Jablonski, A. E.; Kawakami, T.; Ting, A. Y.; Payne, C. K. *J. Phys. Chem. Lett.* **2010**, *1*, 1312–1315.
- (14) (a) Kim, H. J.; Bok, J. H.; Vicens, J.; Suh, I.-H.; Ko, J.; Kim, J. S. *Tetrahedron Lett.* **2005**, *46*, 8765–8768. (b) Ben Othman, A.; Lee, J. W.; Huh, Y.-D.; Abidi, R.; Kim, J. S.; Vicens, J. *Tetrahedron* **2007**, *63*, 10793–10800. (c) Ben Othman, A.; Lee, J. W.; Wu, J. S.; Kim, J. S.; Abidi, R.; Thuéry, P.; Strub, J. M.; Van Dorselaer, A.; Vicens, J. *J. Org. Chem.* **2007**, *72*, 7634–7640. (d) Park, S. Y.; Yoon, J. H.; Hong, C. S.; Souane, R.; Kim, J. S.; Matthews, S. E.; Vicens, J. *J. Org. Chem.* **2008**, *73*, 8212–8218. (e) Kim, H. J.; Hong, J.; Hong, A.; Ham, S.; Lee, J. H.; Kim, J. S. *Org. Lett.* **2008**, *10*, 1963–1966. (f) Leray, I.; Valeur, B. *Eur. J. Inorg. Chem.* **2009**, 3525–3535. (g) Jung, H. S.; Park, M.; Han, D. Y.; Kim, E.; Lee, C.; Ham, S.; Kim, J. S. *Org. Lett.* **2009**, *11*, 3378–3381.
- (15) Yu, C.; Yam, V. W.-W. *Chem. Commun.* **2009**, 1347–1349.
- (16) Lee, Y. H.; Liu, H.; Lee, J. Y.; Kim, S. H.; Kim, S. K.; Sessler, J. L.; Kim, Y.; Kim, J. S. *Chem.—Eur. J.* **2010**, *16*, 5895–5901.
- (17) (a) Suzuki, K.; Seno, A.; Tanabe, H.; Ueno, K. *Synth. Met.* **2004**, *143*, 89–96. (b) Oyamada, T.; Uchiuzou, H.; Akiyama, S.; Oku, Y.; Shimoji, N.; Matsushige, K.; Sasabe, H.; Adachi, C. *J. Appl. Phys.* **2005**, *98*, 074506. (c) Thomas, K. R. J.; Velusamy, M.; Lin, J. T.; Chuen, C. H.; Tao, Y.-T. *J. Mater. Chem.* **2005**, *15*, 4453–4459. (d) Muccini, M. *Nat. Mater.* **2006**, *5*, 605–613. (e) Yang, C.-H.; Guo, T.-F.; Sun, I.-W. *J. Lumin.* **2007**, *124*, 93–98. (f) Zhao, S.-B.; Wucher, P.; Hudson, Z. M.; McCormick, T. M.; Liu, X.-Y.; Wang, S.; Feng, X.-D.; Lu, Z.-H. *Organometallics* **2008**, *27*, 6446–6456. (g) Wee, K.-R.; Ahn, H.-C.; Son, H.-J.; Han, W.-S.; Kim, J.-E.; Cho, D. W.; Kang, S. O. *J. Org. Chem.* **2009**, *74*, 8472–8475. (h) Sonar, P.; Soh, M. S.; Cheng, Y. H.; Henssler, J. T.; Sellinger, A. *Org. Lett.* **2010**, *12*, 3292–3295. (i) Zhou, Y.; Kim, J. W.; Kim, M. J.; Son, W.-J.; Han, S. J.; Kim, H. N.; Han, S.; Kim, Y.; Lee, C.; Kim, S.-J.; Kim, D. H.; Kim, J.-J.; Yoon, J. *Org. Lett.* **2010**, *12*, 1272–1275. (j) for a review on pyrene-based materials for organic electronics, see: Figueira-Duarte, T. M.; Müllen, K. *Chem. Rev.* **2011**, doi: 10.1021/cr100428a.
- (18) Banerjee, M.; Vyas, V. S.; Lindeman, S. V.; Rathore, R. *Chem. Commun.* **2008**, 1889–1891.
- (19) Yang, S.-W.; Elangovan, A.; Hwang, K.-C.; Ho, T.-I. *J. Phys. Chem. B* **2005**, *109*, 16628–16635.
- (20) Venkataramana, G.; Sankararaman, S. *Eur. J. Org. Chem.* **2005**, 4162–4166.
- (21) (a) Leroy-Lhez, S.; Fages, F. *Eur. J. Org. Chem.* **2005**, 2684–2688. (b) Shimizu, H.; Fujimoto, K.; Furusyo, M.; Maeda, H.; Nanai, Y.; Mizuno, K.; Inouye, M. *J. Org. Chem.* **2007**, *72*, 1530–1533.
- (22) Kim, H. M.; Lee, Y. O.; Lim, C. S.; Kim, J. S.; Cho, B. R. *J. Org. Chem.* **2008**, *73*, 5127–5130.
- (23) Wanninger-Weiß, C.; Wagenknecht, H.-A. *Eur. J. Org. Chem.* **2008**, 64–71.
- (24) (a) Astakhova, I. V.; Korshun, V. A. *Russ. J. Bioorg. Chem.* **2008**, *34*, 510–512. (b) Filichev, V. V.; Astakhova, I. V.; Malakhov, A. D.; Korshun, V. A.; Pedersen, E. B. *Chem.—Eur. J.* **2008**, *14*, 9968–9980. (c) Astakhova, I. V.; Lindegaard, D.; Korshun, V. A.; Wengel, J. *Chem. Commun.* **2010**, 46, 8362–8364.
- (25) After our paper was submitted, the following paper appeared: Qiao, Y.; Zhang, J.; Xu, W.; Zhu, D. *Tetrahedron* **2011**, *67*, 3395–3405.
- (26) (a) Runge, E.; Gross, E. K. U. *Phys. Rev. Lett.* **1984**, *52*, 997–1000. (b) Casida, M. E. *Recent Advances in Density Functional Theory: Part I*; World Scientific: Singapore, 1995; pp 155–192.
- (27) Becke, A. D. *J. Chem. Phys.* **1993**, *98*, 5648–5652.
- (28) Lee, C.; Yang, W.; Parr, R. G. *Phys. Rev. B* **1988**, *37*, 785–789.
- (29) Vosko, S. H.; Wilk, L.; Nusair, M. *Can. J. Phys.* **1980**, *58*, 1200–1211.
- (30) Stephens, P. J.; Devlin, F. J.; Chabalowski, C. F.; Frisch, M. J. *J. Phys. Chem.* **1994**, *98*, 11623–11627.
- (31) Yanai, T.; Tew, D. P.; Handy, N. C. *Chem. Phys. Lett.* **2004**, *393*, 51–57.
- (32) (a) Goodpaster, J. V.; Harrison, J. F.; McGuffin, V. L. *J. Phys. Chem. A* **1998**, *102*, 3372–3381. (b) Bito, Y.; Shida, N.; Toru, T. *Chem. Phys. Lett.* **2000**, *328*, 310–315. (c) Parac, M.; Grimme, S. *Chem. Phys. Chem.* **2003**, *292*, 11–21. (d) Grimme, S.; Parac, M. *ChemPhysChem* **2003**, *4*, 292–295. (e) Wang, B.-C.; Chang, J.-C.; Tso, H.-C.; Hsu, H.-F.; Cheng, C.-Y. *J. Mol. Struct.: THEOCHEM* **2003**, *629*, 11–20. (f) Dierksen, M.; Grimme, S. *J. Chem. Phys.* **2004**, *120*, 3544–3554. (g) Park, Y. H.; Cheong, B.-S. *Curr. Appl. Phys.* **2006**, *6*, 700–705. (h) Kerkines, I. S. K.; Petsalakis, I. D.; Theodorakopoulos, G.; Klopper, W. *J. Chem. Phys.* **2009**, *131*, 224315. (i) Bazyl, O. K.; Maier, G. V.; Kopylova, T. N.; Danilova, V. I. *Zh. Prikl. Spekt.* **1982**, *37*, 80–86. (j) Grimme, S.; Neese, F. *J. Chem. Phys.* **2007**, *127*, 154116.
- (33) (a) Matsumi, N.; Naka, K.; Chujo, Y. *J. Am. Chem. Soc.* **1998**, *120*, 5112–5113. (b) Noda, T.; Ogawa, H.; Shirota, Y. *Adv. Mater.* **1999**, *11*, 283–285. (c) Shirota, Y.; Kinoshita, M.; Noda, T.; Okumoto, K.; Ohara, T. *J. Am. Chem. Soc.* **2000**, *122*, 11021–11022. (d) Entwistle, C. D.; Marder, T. B. *Angew. Chem., Int. Ed.* **2002**, *41*, 2927–2931 and references therein. (e) Entwistle, C. D.; Marder, T. B. *Chem. Mater.* **2004**, *16*, 4574–4585. (f) Qin, Y.; Cheng, G.; Achara, O.; Parab, K.; Jäkle, F. *Macromolecules* **2004**, *37*, 7123–7131. (g) Parab, K.; Qin, Y.; Haleem, S.; Jäkle, F. *Polym. Mater. Sci. Eng. Prepr.* **2005**, *93*, 422–423. (h) Liu, X. Y.; Bai, D. R.; Wang, S. *Angew. Chem., Int. Ed.* **2006**, *45*, 5475–5478. (i) Jäkle, F. *Coord. Chem. Rev.* **2006**, *250*, 1107–1121. (j) Wakamiya, A.; Mori, K.; Yamaguchi, S. *Angew. Chem., Int. Ed.* **2007**, *46*, 4273–4276. (k) Haussler, M.; Tang, B. Z. *Adv. Polym. Sci.* **2007**, *209*, 1–58. (l) Elbing, M.; Bazan, G. C. *Angew. Chem., Int. Ed.* **2008**, *47*, 834–838.
- (34) (a) Yuan, Z.; Taylor, N. J.; Marder, T. B.; Williams, I. D.; Kurtz, S. K.; Cheng, L.-T. *J. Chem. Soc., Chem. Commun.* **1990**, 1489–1492. (b) Yuan, Z.; Taylor, N. J.; Marder, T. B.; Williams, I. D.; Kurtz, S. K.; Cheng, L.-T. In *Organic Materials for Non-linear Optics II*; Hann, R. A., Bloor, D., Eds.; Royal Society of Chemistry: Cambridge, U.K., 1991; pp 190–196. (c) Yuan, Z.; Taylor, N. J.; Sun, Y.; Marder, T. B.; Williams, I. D.; Cheng, L.-T. *J. Organomet. Chem.* **1993**, *449*, 27–37. (d) Yuan, Z.; Taylor, N. J.; Ramachandran, R.; Marder, T. B. *Appl. Organomet. Chem.* **1996**, *10*, 305–316. (e) Yuan, Z.; Collings, J. C.; Taylor, N. J.; Marder, T. B.; Jardin, C.; Halet, J.-F. *J. Solid State Chem.* **2000**, *154*, 5–12. (f) Yuan, Z.; Entwistle, C. D.; Collings, J. C.; Albesa-Jové, D.; Batsanov, A. S.; Howard, J. A. K.; Kaiser, H.-M.; Kaufmann, D. E.; Poon, S.-Y.; Wong, W.-Y.; Jardin, C.; Fathallah, S.; Boucekkine, A.; Halet, J.-F.; Marder, T. B. *Chem.—Eur. J.* **2006**, *12*, 2758–2771. (g) Zhou, G.; Ho, C.-L.; Wong, W.-Y.; Wang, Q.; Ma, D.; Wang, L.; Lin, Z.; Marder, T. B.; Beeby, A. *Adv. Funct. Mater.* **2008**, *18*, 499–511. (h) Weber, L.; Werner,

- V.; Fox, M. A.; Marder, T. B.; Schwedler, S.; Brockhinke, A.; Stammer, H.-G.; Neumann, B. *Dalton Trans.* **2009**, 2823–2831. (i) Braunschweig, H.; Herbst, T.; Rais, D.; Ghosh, S.; Kupfer, T.; Radacki, K.; Crawford, A. G.; Ward, R. M.; Marder, T. B.; Fernández, I.; Frenking, G. *J. Am. Chem. Soc.* **2009**, *131*, 8989–8999.
- (35) (a) Charlot, M.; Porrès, L.; Entwistle, C. D.; Beeby, A.; Marder, T. B.; Blanchard-Desce, M. *Phys. Chem. Chem. Phys.* **2005**, *7*, 600–606. (b) Porrès, L.; Charlot, M.; Entwistle, C. D.; Beeby, A.; Marder, T. B.; Blanchard-Desce, M. *Proc. SPIE—Int. Soc. Opt. Eng.* **2005**, *92*, 5934–5936. (c) Collings, J. C.; Poon, S.-Y.; Le Droumaguet, C.; Charlot, M.; Katan, C.; Pålsson, L.-O.; Beeby, A.; Mosely, J. A.; Kaiser, H.-M.; Kaufmann, D.; Wong, W.-Y.; Blanchard-Desce, M.; Marder, T. B. *Chem.—Eur. J.* **2009**, *15*, 198–208. (d) Entwistle, C. D.; Collings, J. C.; Steffen, A.; Pålsson, L.-O.; Beeby, A.; Albesa-Jové, D.; Burke, J. M.; Batsanov, A. S.; Howard, J. A. K.; Mosely, J. A.; Poon, S.-Y.; Wong, W.-Y.; Ibersiene, F.; Fathallah, S.; Boucekkine, A.; Halet, J.-F.; Marder, T. B. *J. Mater. Chem.* **2009**, *40*, 7532–7544.
- (36) (a) Stolka, M.; McGrane, K. M.; Facci, J. S. Photoconductive Imaging Members with Alkoxy Amine Charge Transport Molecules. U.S. Patent 4,588,666, May 13, 1986. (b) Bellmann, E.; Shaheen, S. E.; Thayumanavan, S.; Barlow, S.; Grubbs, R. H.; Marder, S. R.; Kippelen, B.; Peyghambarian, N. *Chem. Mater.* **1998**, *10*, 1668–1676. (c) Mitschke, U.; Bäuerle, P. *J. Mater. Chem.* **2000**, *10*, 1471–1507. (d) Low, P. J.; Paterson, M. A. J.; Puschmann, H.; Goeta, A. E.; Howard, J. A. K.; Lambert, C.; Cherryman, J. C.; Tackley, D. R.; Leeming, S.; Brown, B. *Chem.—Eur. J.* **2004**, *10*, 83–91. (e) Bardecker, J. A.; Ma, H.; Kim, T.; Huang, F.; Liu, M. S.; Cheng, Y.-J.; Ting, G.; Jen, A. K.-Y. *Adv. Funct. Mater.* **2008**, *18*, 3964–3971.
- (37) (a) Nguyen, P.; Yuan, Z.; Agocs, L.; Lesley, G.; Marder, T. B. *Inorg. Chim. Acta* **1994**, *220*, 289–296. (b) Khan, M. S.; Kakkar, A. K.; Long, N. J.; Lewis, J.; Raithby, P.; Nguyen, P.; Marder, T. B.; Wittmann, F.; Friend, R. H. *J. Mater. Chem.* **1994**, *4*, 1227–1232. (c) Nguyen, P.; Lesley, G.; Marder, T. B.; Ledoux, I.; Zyss, J. *Chem. Mater.* **1997**, *9*, 406–408. (d) Biswas, M.; Nguyen, P.; Marder, T. B.; Khundkar, L. R. *J. Phys. Chem. A* **1997**, *101*, 1689–1695. (e) Li, H.; Powell, D. R.; Firman, T. K.; West, R. *Macromolecules* **1998**, *31*, 1093–1098. (f) Bunz, U. H. F. *Chem. Rev.* **2000**, *100*, 1605–1644. (g) Donhauser, Z. J.; Mantooth, B. A.; Kelly, K. F.; Bumm, L. A.; Monnell, J. D.; Stapleton, J. J.; Price, D. W., Jr.; Rawlett, A. M.; Allara, D. L.; Tour, J. M.; Weiss, P. S. *Science* **2001**, *292*, 2303–2307. (h) Dirk, S. M.; Price, D. W., Jr.; Chanteau, S.; Kosynkin, D. V.; Tour, J. M. *Tetrahedron* **2001**, *57*, 5109–5121. (i) Kim, J.; Swager, T. M. *Nature* **2001**, *411*, 1030–1034. (j) Schmitz, C.; Pösch, P.; Thelakkat, M.; Schmidt, H.-W.; Montali, A.; Feldman, K.; Smith, P.; Weder, C. *Adv. Funct. Mater.* **2001**, *11*, 41–46. (k) Levitus, M.; Schmieder, K.; Ricks, H.; Shimizu, K. D.; Bunz, U. H. F.; Garcia-Garibay, M. A. *J. Am. Chem. Soc.* **2001**, *123*, 4259–4265. (l) Beeby, A.; Findlay, K. S.; Low, P. J.; Marder, T. B.; Matousek, P.; Parker, A. W.; Rutter, S. R.; Towrie, M. *Chem. Commun.* **2003**, 2406–2407.
- (38) (a) Nakatsuji, S.; Matsuda, K.; Uesugi, Y.; Nakashima, K.; Akiyama, S.; Fabian, W. *J. Chem. Soc., Perkin Trans. I* **1992**, *7*, 755–758. (b) Nguyen, P.; Todd, S.; van den Biggelaar, D.; Taylor, N. J.; Marder, T. B.; Wittmann, F.; Friend, R. H. *Synlett* **1994**, 299–301. (c) Kawai, T.; Sasaki, T.; Irie, M. *Chem. Commun.* **2001**, 711–712. (d) Schmieder, K.; Levitus, M.; Dang, H.; Garcia-Garibay, M. A. *J. Phys. Chem. A* **2002**, *106*, 1551–1556. (e) Giménez, R.; Piñol, M.; Serrano, J. L. *Chem. Mater.* **2004**, *16*, 1377–1383. (f) Beeby, A.; Findlay, K. S.; Goeta, A. E.; Porrès, L.; Rutter, S. R.; Thompson, A. L. *Photochem. Photobiol. Sci.* **2007**, *6*, 982–986.
- (39) (a) Siddle, J. S.; Ward, R. M.; Collings, J. C.; Rutter, S. R.; Porrès, L.; Applegarth, L.; Beeby, A.; Batsanov, A. S.; Thompson, A. L.; Howard, J. A. K.; Boucekkine, A.; Costuas, K.; Halet, J.-F.; Marder, T. B. *New J. Chem.* **2007**, *31*, 841–851. (b) Matano, Y.; Nakashima, M.; Imahori, H. *Angew. Chem., Int. Ed.* **2009**, *48*, 4002–4005. (c) Steffen, A.; Tay, M. G.; Batsanov, A. S.; Howard, J. A. K.; Beeby, A.; Vuong, K. Q.; Sun, X.-Z.; George, M. W.; Marder, T. B. *Angew. Chem., Int. Ed.* **2010**, *49*, 2349–2353.
- (40) Mkhaliid, I. A. I.; Barnard, J. H.; Marder, T. B.; Murphy, J. M.; Hartwig, J. F. *Chem. Rev.* **2010**, *110*, 890–931.
- (41) (a) Yoshinaga, T.; Hiratsuka, H.; Tanizaki, Y. *Bull. Chem. Soc. Jpn.* **1977**, *50*, 3096–3102. (b) Turro, N. J.; Ramamurthy, V.; Scaiano, J. C. *Principles of Molecular Photochemistry, An Introduction*; University Science Books: Sausalito, CA, 2009. (c) Birks, J. B. *Photophysics of Aromatic Molecules*; Wiley-Interscience: London, 1970. (d) Values measured by the authors. (e) Michl, J.; Thulstrup, E. W. *Spectroscopy with Polarized Light*; VCH Publishers Inc.: New York, 1986; p 368. (f) Klessinger, M.; Michl, J. *Excited States and Photochemistry of Organic Molecules*; Wiley-VCH: New York, 1995; Chapters 1 and 2.
- (42) Clar, E. *Polycyclic Hydrocarbons*; Academic Press: London, 1964.
- (43) (a) Platt, J. R. *J. Chem. Phys.* **1949**, *17*, 484–495. (b) Platt, J. R. *J. Opt. Soc. Am.* **1953**, *43*, 252–257. (c) Moffitt, W. *J. Chem. Phys.* **1954**, *22*, 320–333.
- (44) Nakajima, A. *Bull. Chem. Soc. Jpn.* **1971**, *44*, 3272–3277.
- (45) Foggi, P.; Pettini, L.; Santa, I.; Righini, R.; Califano, S. *J. Phys. Chem.* **1995**, *99*, 7439–7445.
- (46) Iikura, H.; Tsuneda, T.; Yanai, T.; Hirao, K. *J. Chem. Phys.* **2001**, *115*, 3540–3544.
- (47) Peach, M. J. G.; Benfield, P.; Helgaker, T.; Tozer, D. J. *J. Chem. Phys.* **2008**, *128*, 044118.
- (48) Wiggins, P.; Williams, J. A. G.; Tozer, D. J. *J. Chem. Phys.* **2009**, *131*, 091101.
- (49) “Pyrene-like”: This descriptor refers to transitions that occur between orbitals similar to the HOMO and LUMO in pyrene, i.e., the $S_2 \leftarrow S_0$ transition in pyrene (Figure 4).
- (50) “Substituent-influenced”: This descriptor refers to transitions that occur between orbitals similar to the HOMO – 1/HOMO and LUMO/LUMO + 1 in pyrene, i.e., the $S_1 \leftarrow S_0$ transition in pyrene (Figure 4).
- (51) (a) Beeby, A.; Findlay, K.; Low, P. J.; Marder, T. B. *J. Am. Chem. Soc.* **2002**, *124*, 8280–8284. (b) Greaves, S. J.; Flynn, E. L.; Fletcher, E. L.; Wrede, E.; Lydon, D. P.; Low, P. J.; Rutter, S. R.; Beeby, A. *J. Phys. Chem. A* **2006**, *110*, 2114–2121.
- (52) Weber, L.; Werner, V.; Fox, M. A.; Marder, T. B.; Schwedler, S.; Brockhinke, A.; Stammer, H.-G.; Neumann, B. *Dalton Trans.* **2009**, 1339–1351.
- (53) Porrès, L.; Holland, A.; Pålsson, L.-O.; Monkman, A. P.; Kemp, C.; Beeby, A. *J. Fluoresc.* **2006**, *16*, 267–272.
- (54) O’Connor, D. V.; Phillips, D. *Time-correlated Single Photon Counting*; Academic Press: New York, 1984.
- (55) Frisch, M. J.; et al. *Gaussian 03*, revision C.02; Gaussian, Inc.: Wallingford, CT, 2004. The complete reference is given in the Supporting Information.
- (56) Dalton, a molecular electronic structure program, release 2.0, 2005; see <http://www.kjemi.uio.no/software/dalton/dalton.html>.